Nucleonic Design for a Compact Tokamak Fusion Reactor Blanket and Shield

E.T. Cheng, C.W. Maynard, W.F. Vogelsang, and A.C. Klein

August 1978

UWFDM-256

Nucl. Tech. 45, 77 (1979).

FUSION TECHNOLOGY INSTITUTE

UNIVERSITY OF WISCONSIN

MADISON WISCONSIN

Nucleonic Design for a Compact Tokamak Fusion Reactor Blanket and Shield

E.T. Cheng, C.W. Maynard, W.F. Vogelsang, and
A.C. Klein

Fusion Technology Institute
University of Wisconsin
1500 Engineering Drive
Madison, WI 53706

http://fti.neep.wisc.edu

August 1978

UWFDM-256

Nucl. Tech. 45, 77 (1979).

Nucleonic Design for a Compact Tokamak Fusion Reactor Blanket and Shield†

E.T. Cheng*
C.W. Maynard
W.F. Vogelsang
and
A.C. Klein

Nuclear Engineering Department
University of Wisconsin
Madison, Wisconsin 53706

UWFDM-256

August 1978

†Research supported in part by the Department of Energy and Wisconsin Electric Utilities Research Foundation

*Present address: General Atomic Company P.O. Box 81608, San Diego CA 92138

Abstract

An optimization study of the nucleonic design of the blanket and shield for a compact tokamak fusion reactor is given. One of the characteristics of such a compact reactor is high power density (~ 10 MW/m^3) and thus high neutron wall loading (~ 5 MW/m^2). The most crucial design requirements for a tokamak fusion reactor blanket and shield are: adequate tritium breeding ratio (> 1.10); high blanket energy multiplication ($\geq$ 1.2); adequate magnet protection; and low radioactivity. The magnet protection criterion for a compact reactor is particularly essential in the inner region of the torus close to the toroidal axis because of limited space availability for shielding. A very effective shielding material such as tungsten must be used for this purpose. The design requirements have been satisfied by the selection of blanket and shielding materials as well as their zone thicknesses and heights. In this paper, a compact tokamak fusion reactor, NUWMAK, is studied. A tritium breeding ratio of 1.54 is obtained. $Li_{62}Pb_{38}$ eutectic is used as the breeding and thermal energy storage material. The total nuclear heating in the blanket and shield is ~ 17.2 MeV per D-T neutron. The performance of the superconducting magnet will be satisfactory for more than two years of continuous operation through the use of a tungsten shield 35 cm thick and extending 2.5 m above the midplane on the in board part of the torus. The radioactivity is lowered by using a titanium alloy as the structural material and large amounts of lithium lead as the blanket material. One day after shutdown, the dose rate outside the outer shield drops below 2.6 mrem per hour and it is favorable to hands on shift maintenance.

I. Introduction

A compact tokamak fusion reactor design[1] has evolved from the series of UWMAK designs, namely UWMAK-I,[2] II[3] and III.[4] This new conceptual design, the NUWMAK, is characterized by a high value of plasma power density (11 MW/m^3) and spatially averaged neutron wall loading (4.34 MW/m^2). It has a major and minor radius of 5.13 and 1.13 meters, respectively, and a height to width ratio of 1.64. The on-axis magnetic field is 6.05 tesla and maximum field at the magnet is 11.5 tesla. There are only eight superconducting coils in this design and this provides extensive space for access and maintenance.[5] The major features and cross sectional view of the NUWMAK design are tabulated and depicted in Table 1 and Fig. 1 respectively.

In this paper we present the nucleonic design for the NUWMAK blanket and shield. The general design goals for this type of compact reactor are as follows: A tritium breeding ratio of no less than 1.10; a blanket/shield energy deposition of no less than 17 MeV per D-T neutron; the maximum resistivity change in the superconducting stabilizer and the critical current density change in the superconductors are smaller than 50% and 2%, respectively; an endurable dose on the superinsulators for the entire plant lifetime; and low radioactivity. All the above considerations are discussed in detail in Sec. II. Sec. III presents methods of neutronic calculations and analyses which include one and two dimensional problems. In Sec. IV preliminary survey and design calculations are given in which the tritium breeding ratio as a function of lithium lead composition and percent ^6Li in total lithium are considered. This section includes magnet protection considerations, discussing each

shield zone thickness and height. The final results for the NUWMAK blanket and shield design are presented in Sec. V. The discussion of radioactivity, afterheat, biological hazard potential (BHP) and dose rate after shutdown is given in Sec. VI. Finally, the conclusions of this nucleonic design for a compact tokamak fusion reactor blanket and shield are summarized in Sec. VII.

II. Design Goals for NUWMAK Blanket and Shield

The design goals for the NUWMAK blanket and shield have evolved from our previous conceptual tokamak fusion reactor designs[2-4] and from those discussed in the literature[7-12]. Here, we will briefly review some of the important features related to the blanket and shield design and summarize the design requirements on the characteristic roles of the blanket and shield, namely, tritium breeding, nuclear energy deposition and magnet shielding.

II.A. Tritium Breeding

It has been shown that a tritium breeding ratio of ~1.02 tritons per D-T neutron is capable of producing a doubling time of 2-7 years[7]. This means that a tritium breeding ratio of slightly greater than unity would meet the refueling requirement of a D-T fusion reactor for the whole plant lifetime of about 30 years. However, considering the uncertainties inherent in the neutron transport calculation due to the geometric homogeneity assumed in the calculational model, and the nuclear data uncertainty, it is very often required that the tritium breeding ratio is to be greater than 1.10 in order to assure the adequacy of the breeding capability[8].

II.B. Nuclear Energy Deposition

One of the basic functions of the blanket is to intercept the 14 MeV neutrons and convert their kinetic energy into heat. The blanket energy multiplication, M, is given by the ratio of the heat deposited in the blanket to the source neutron kinetic energy, i.e.,

$$M = \frac{\text{Blanket Heat Deposition (MeV per D-T Neutron)}}{\text{Source Neutron Energy (14.1 MeV per Neutron)}}$$

In order to obtain a higher thermal power output, the blanket energy multiplication is to be as large as possible. It is desired that $M \geq 1.2$, i.e., the blanket heat deposition is greater than 17 MeV per D-T fusion neutron. Since the heat deposited in the cold shield will not be recoverable, this heat should be designed to be as small as possible. In this study we have limited the non-recoverable heat to less than one percent of the total thermal output.

II.C. Magnet Shielding

In a fusion reactor shield design, the most severe problem is to protect the superconducting magnet. The function of a superconducting magnet can be affected during reactor operation through radiation damage to the magnet components, namely, superconductors, structural, stabilizing, and superinsulating materials.

In the superconductors, the radiation damage is primarily due to neutron bombardment and affects the critical temperature, T_c, and the critical current density, J_c. It has been reported that the reduction of T_c in NbTi is very small under a neutron fluence of 10^{18} n/cm^2. The reduction of J_c in NbTi is less than 0.5% if the irradiating neutron fluence is no more than 10^{17} n/cm^2. However, it will be more than 16% or 170% if the neutron fluence is 5×10^{18} or 10^{19} n/cm^2 respectively[9].

As far as the stabilizing material is concerned, the radiation damage results in an increase of the electrical resistivity under neutron irradiation. For the aluminum stabilizer studied here the electrical resistivity is not sensitive to an applied magnetic field of more than 2

tesla[10]. The neutron irradiation effect is measured by the extent of atomic displacement (displacement per atom, dpa) in metals. For an atomic displacement of 10^{-5} dpa, the resistivity will increase by $\sim 1.3 \times 10^{-8}$ ohm-cm, which is ~1.3 times that of the resistivity without irradiation*. However, the increase of the electrical resistivity is ~13% if the atomic displacement is $\sim 1 \times 10^{-6}$ dpa. The resistivity change below 10^{-5} dpa is roughly linear and can be expressed as

$$\rho_c = 1.33 \times 10^{-3} \times \text{dpa (ohm - cm) for dpa} \leq 10^{-5} .$$

For the design of a superconducting magnet the magnetic field strength and the heat transfer characteristics are very important considerations during operation. The magnetic field strength and the ohmic heat generation are proportional to the current density in the superconductors and the resistivity in the stabilizer, respectively. Hence, the reduction of the critical current density in the superconductor, as well as the increase of the resistivity in the stabilizer will limit as well as determine the functioning of the magnet. However, the resistivity change and critical current density reduction are recoverable as the magnet is brought back to higher temperature for annealing. For example, the recovery of the aluminum resistivity is almost 100% at room temperature[10]. Thus it is very important to expect a reasonable period of down time for both blanket replacement and magnet annealing in order to maximize the plant utilization.

In the design of the NUWMAK magnet, a maximum increase of 50% for the resistivity in the aluminum stabilizer is used as the limit. As the value of resistivity reaches this limit, the plant will be shut down and the

*The electrical resistivity of the aluminum adopted in the UWMAK-III (Ref. 4) and NUWMAK designs is 1×10^{-8} ohm-cm. This is higher than the predicted value, $\sim 7 \times 10^{-9}$ ohm-cm, for safety purpose.

magnet annealed while the blanket is replaced. Corresponding to this limit, ~4 x 10^{-6} dpa at the aluminum stabilizer is expected.

While the radiation damage to the superconductors and stabilizer can be restored, the effects on the superinsulation materials are irreversible[11]. Radiation damage to the superinsulation materials is measured in terms of the dose or the amount of nuclear energy, including neutron and gamma-ray, absorbed in them expressed in units of rads (one rad is defined as the absorption of 100 ergs of energy by a gram of material mass). It has been reported[11,12] that mylar based superinsulators suffer severe property changes if the dose is more than 1 x 10^8 rads. However, the endurable dose for epoxy based superinsulators is in the range of 1-5 x 10^9 rads. Therefore, for a plant lifetime of ~30 years, a dose rate of less than 3 x 10^6 and 3-15 x 10^7 rads/year is desired if mylar and epoxy based superinsulators are to be employed for the magnet design.

In summary, in the design of the NUWMAK blanket and shield, we aim at the following criteria:

1. A tritium breeding ratio of no less than 1.10 tritons per D-T neutron.
2. A blanket/shield energy deposition of no less than 17 MeV per D-T neutron, of which ~99% is recoverable.
3. The maximum resistivity change in the aluminum stabilizer and the critical current density reduction in the superconductors are no greater than 50% and 2%, respectively, before magnet annealing takes place.
4. An endurable dose to the superinsulation materials for the plant lifetime.

III. Methods of Calculation

The neutronics calculations make use of one and two-dimensional discrete ordinates transport codes, ANISN[13] and DØT[14] for either survey or design purposes. The calculations were performed with the P_3S_4 approximation in cylindrical or r-z geometry depending on whether one or two dimensional models are used. The nuclear cross section library used is the same as described elsewhere[15] and is collapsed into coupled 25 neutron and 21 gamma-ray groups. In Table II the neutron group structure is given and compared to that from Ref. 15. The gamma-ray group structure is kept unchanged. The displacement cross sections were obtained from Ref. 16. The neutronics model, which is used to provide detailed spatial neutron and gamma-ray fluxes and nuclear responses, consists of the important components of fusion reactors; namely the magnet, the shield, the blanket, and the plasma and vacuum core. Two dimensional models, as shown in Fig. 2, provide for the poloidal variation in zone thicknesses and the different design of the inner shield. The blanket and shield are made of the titanium alloy, Ti-6242. The piping material is another titanium alloy, Ti-6Al-4V. However, in the flux calculations, both structural and piping materials are treated as the alloy, Ti-6Al-4V, and this has almost no effect on the neutronic results. The coolant is boiling water. At the midplane, the inner blanket/shield consists of a 20 cm breeding zone, a tungsten hot shield, a boron carbide cold shield and a lead zone. The individual zone thickness is to be decided after an analysis of the survey calculations according to the design goals discussed in the previous section. The total thickness of this shield zone is fixed at 85 cm. Thus, the distance from the first wall to the dewar of the superconducting coils is only 1.05 meters. The outer blanket/shield region

consists of a 50 cm breeding blanket, a 20 cm graphite reflector and a boron carbide cold shield thick enough to protect the magnet close to the outer portion of the torus. Note the blanket zones are divided into several (five as shown in Table IV) subzones to account for various amounts of structure/piping and coolant inferred from nuclear heating distributions (two and three subzones for inner and outer blankets, respectively). The volume present for the structure/piping ranges from 12 to 4% as one moves through the blanket region away from the first wall. The volume percent for the coolant ranges from 9 to 2%. The breeding material thus varies from 79 to 94% by volume. As discussed in Ref. 6, the lithium lead eutectic $Li_{62}\ Pb_{38}$ is employed as the breeding material. The advantages resulting from the use of this eutectic are twofold. One is that it will be easy to obtain a tritium breeding ratio greater than 1.10, as will be discussed later. The other is that this blanket will provide an internal energy storage through its phase change during plasma burn and down time by operating the blanket at a temperature around the melting temperature of the $Li_{62}\ Pb_{38}$ eutectic, 464°C. The solid and liquid (at 500°C which is the maximum operating temperature in the blanket) densities for this $Li_{62}\ Pb_{38}$ eutectic are estimated to be 6.5 and 5.0 g/cm^3 respectively. The volume fraction of these two phases during blanket operation is roughly equal[6], hence the average value of these two densities is taken as the calculational $Li_{62}\ Pb_{38}$ density in this study. As for the density of each shield material, from the present attainable technology, density factors of 0.9, 0.9 and 0.95 are taken into consideration when tungsten, lead and boron carbide are employed. The average density for the boiling water in each zone is estimated and used in the calculation.

IV. Survey Calculations and Discussions

In this section, we present and discuss results of several survey calculations. The computational results for the final design of NUWMAK are given in the next section.

Based on the design goals described in Sec. II, we investigate here the tritium breeding, nuclear heating and the magnet shielding arrangement. However, two of the most important design criteria which are sensitive to the design variations will be emphasized in this study. One is the tritium breeding, in which we study the tritium breeding potential of the lithium lead compositions, such as $LiPb_4$, LiPb and $Li_{62}Pb_{38}$. The sensitivity to the percent ^6Li in total lithium in the $Li_{62}Pb_{38}$ eutectic chosen for this blanket breeding material of the tritium breeding is also studied. The other is the magnet shielding arrangement in which we look at the effect on the magnet damage responses of the thickness for each shield material zone in the inner shield region, namely tungsten, B_4C and the lead zone (for a fixed total thickness of 85 cm). The effect of the height of the tungsten zone is also considered.

IV.A. Tritium Breeding vs. Lithium Lead Composition

The choice of the $Li_{62}Pb_{38}$ eutectic as the breeding material is mainly based on thermal design considerations[6]. Its melting temperature, 464°C, coupled with the use of Ti-6Al-4V alloy as piping/structural material, which operates best in the range of 300-390°C, makes it a suitable blanket material for high thermal efficiency and for providing internal energy storage to minimize the thermal cycling and eliminate external storage. Nevertheless, it is of interest to investigate the tritium breeding potential over the various compositions of the lithium lead alloys or eutectics. For simplicity we fix all the

alloys at 500°C and use the ideal solution approximation to estimate their densities. In Table III, a list of solid and liquid (500°C) densities for several lithium lead alloys is given for comparison. At practical operating conditions, the tritium breeding ratio may be expected to be no less than obtained in this study.

Fig. 3 shows the tritium breeding ratio as a function of the lithium (natural lithium) atom percent in lithium lead alloys. It is found in this figure that as the atomic percent lithium in the lithium lead alloy is not less than 20%, i.e., $LiPb_4$, the tritium breeding ratio is adequately bracketed between 1.45 and 1.55 tritons per D-T neutron. At 100% lithium atom percent, i.e., pure lithium, it is ~1.46 which is about the same as found in the UWMAK-I design. The resulting approximately constant tritium breeding is primarily due to the competition between $^7Li(n,n'\alpha)T$ and Pb(n,2n) reactions, while all the secondary neutrons are absorbed by ^6Li and result in production of additional tritons. This can be easily revealed by comparing the contribution from the $^6Li(n,\alpha)T$ (T_6) and $^7Li(n,n'\alpha)T$ (T_7) reactions shown in Fig. 3.

IV.B. Tritium Breeding vs. Percent ^6Li in Total Lithium

Natural lithium consists of only 7.42% of ^6Li. Percent of ^6Li other than the natural content in total lithium has been employed in reactor blanket design[3]. In this subsection we will discuss the effect of the percent ^6Li in total lithium on the tritium breeding ratio.

Due to thermal design considerations, we choose $Li_{62}Pb_{38}$ eutectic as the tritium breeding and nuclear energy deposition material in the blanket. Here we will also employ this candidate eutectic in this study although the results may be equally applicable to most lithium lead alloys

whose tritium breeding potential were discussed in Sec. IV.A. Note the $Li_{62}Pb_{38}$ density used here is the average value of solid and liquid densities as will be used in the final design calculations. Fig. 4 shows the calculational results. The maximum tritium breeding ratio, ~1.64 tritons per D-T neutron, is obtained at ~30% ^6Li in total lithium. However, at 7.42% ^6Li (natural lithium) and 90% ^6Li, the tritium breeding ratios are very close, 1.54 and 1.51 tritons per D-T neutron, respectively. The contribution from T_6 increases from 90 to more than 99% as the ^6Li in total lithium increases from 7.42 to 90%. It is noticed that the increase of the tritium breeding ratio from that of the natural-lithium lead eutectic blanket to the maximum value is only 6%. The blanket spatial distribution of the tritium breeding at the midplane for 7.42, 30 and 90% ^6Li in total lithium are depicted in Fig. 5.

From the above considerations, we conclude that there is no incentive to increase the percent ^6Li in total lithium in the lithium lead eutectic for tritium breeding purposes.

IV.C. Magnet Protection Considerations

The NUWMAK magnet system consists of NbTi superconductors, aluminum stabilizer and structure, and superinsulation. The superconductor operates at 1.8°K and is cryogenically cooled by superfluid helium. Due to the design space requirements for the magnet and the plasma ohmic heating coils, the minimum space available for the magnet shielding appears at the midplane close to the toroidal axis (inner blanket/shield region) and is only 1.05 meters from the plasma chamber first wall to the dewar of the magnet. Excluding 20 cm for the blanket zone, a space of only 85 cm is actually available to provide adequate shielding for the protection of the superconducting magnet from the environment of intense nuclear radiation (~5 MW/m^2 neutron wall loading). Although the existence of large amounts

of lead in the Li_{62} Pb_{38} eutectic in the inner blanket provides a good attenuation of the D-T neutrons through (n,2n) and inelastic scattering reactions, metallic tungsten is essential for effectively attenuating both high energy neutron and gamma radiations coming through the blanket. The lowest threshold energies for (n,2n) and inelastic reactions among the tungsten isotopes existing in nature are 6.3 MeV and 46.7 keV for ^{183}W, respectively. These values are comparatively lower than those of other candidate materials such as Fe, Nb, Mo and Pb. Moreover, the macroscopic interaction cross section, which is directly related to the attenuation of neutron radiation, depends on the atomic density of the material. Tungsten metal is a relatively dense material as far as high atomic mass number materials are concerned with an atomic density of 0.0629×10^{24} atoms/cm^3 as compared to 0.03348×10^{24} atoms/cm^3 for lead.

The secondary neutrons coming through the blanket are energetically peaked in the range 0.74 - 2.5 MeV (groups 15-17 in the 25 neutron group structure). The mean free path due to inelastic scattering processes for neutrons of this energy range in the tungsten material is ~8 cm, which is about one half of that in iron, niobium and molybdenum, and about one fourth of that in lead. However, for source neutrons (14 MeV energy), the overall mean free path in tungsten is ~3 cm, which is less than 80% of that in comparable materials. Nevertheless, the neutron energy and particle attenuation depend on the actual neutron spectrum and the composition of the medium, and the attenuation process is too complicated to be fully described by partial or even total interaction cross sections. The solution must be obtained from transport calculations or experimental

measurements depending on the attenuation goal. In order to quantitatively describe the superiority of the use of tungsten metal as the most effective shielding material, we completed several transport calculations. The shielding materials considered here are stainless steel (SS), lead (Pb) and tungsten (W) mixed with boron carbide (B_4C). The composition used is the same as was reported in Ref. 17 as being the best energy attenuating shielding composition for metal and B_4C mixtures, i.e., 70% metal and 30% B_4C by volume. From these calculations, we found that for the same amount of radiation attenuation for atomic displacement rate and neutron fluence in the magnet, SS + B_4C and Pb + B_4C zones needed to be ~50% thicker than a W + B_4C mixture. The maximum atomic displacement rate at the aluminum stabilizer is required to be of the order of 10^{-6} dpa/year while it is more than 100 dpa/year at the first wall. More than seven orders of magnitude attenuation is required for the atomic displacement rate from the back of blanket to the magnet assuming one order of magnitude is achieved by the 20 cm blanket region. It seems that tungsten is the only candidate for the design of the magnet shield described above[18].

IV.C.1. Tungsten Zone Thickness vs. Atomic Displacement Rate in Aluminum Stabilizer

In the following survey calculations, tungsten and B_4C will be employed to study the attenuation effectiveness as a function of tungsten zone thickness. However, the tungsten metal is put before the B_4C shield in order to efficiently utilize its high energy attenuation property and to decrease the total amount of tungsten in the shield design because of its expensiveness.

Fig. 6 shows the atomic displacement rate in the aluminum stabilizer as a function of the tungsten zone thickness. Note here the total thickness for the shield material is 85 cm and a lead zone of 5 cm is already taken into account for the purpose of decreasing the nuclear dose in the superinsulation as well as the whole magnet. In this figure, it is found that the minimum radiation damage level to the aluminum stabilizer is $\sim 2 \times 10^{-7}$ dpa/year at ~55 cm of tungsten zone thickness. Using a tungsten zone thicker than this value, the radiation damage level increases rather than decreasing further. The reason is primarily that the remaining B_4C zone is not thick enough and does not absorb enough of the neutrons. For a tungsten zone of between 35 and 40 cm, the value for the atomic displacement rate in the aluminum stabilizer lies between $\sim 2 \times 10^{-6}$ and 1×10^{-6} dpa/year, which will cause a resistivity increase of between ~25 and 13% after one year of operation.

IV.C.2. Lead Zone Thickness vs. Dose and Atomic Displacement Rates

From the results discussed in the previous subsection, reasonable tungsten zone thickness is found to be between 35 and 40 cm. In order to know more about the dose rate on the superinsulator as well as the magnet, the lead zone thickness is varied for these two designs. The results are shown in Fig. 7, where the atomic displacement rate ranges from 1×10^{-6} and 2×10^{-6} to 1.8×10^{-6} and 3×10^{-6} dpa/year as the lead zone increases from 5 to 10 cm for the design of a tungsten zone of 40 and 35 cm, respectively.

However, the dose rate on the superinsulator will be about three times less as the lead zone increases from 5 cm to 10 cm. For a 5 cm lead zone thickness, the dose rate on the superinsulator is about 3×10^7 and 1.7×10^7 rads/year for the design with a 35 and 40 cm tungsten zone, respectively. As far as the heat load on the magnet is concerned, it increases from ~60 to 515 watts* as the lead zone thickness decreases from 10 to 5 cm. However, this amount of heat is still small compared to the total heat generated and being transferred from the magnet system.

IV.C.3. Tungsten Zone Height vs. Atomic Displacement, Dose Rate and Neutron Fluence

The importance of the radiation protection is not only for the superconducting magnet at the midplane region but also for the entire magnet. It is very necessary to look at the radiation damage for the magnet region close to the plasma as a function of height above the midplane, for the magnet region shown in Fig. 2. A survey study is given here for the case of a 35 cm tungsten zone with a 5 cm lead zone. The height of the tungsten zone is varied from 2 to 2.5 meters for survey purposes.

Figs. 8-10 show the results of these calculations. In these figures, the atomic displacement rate in the aluminum stabilizer, the maximum neutron fluence and dose rate on the superinsulator as a function of magnet region height above the midplane are presented for the cases of tungsten zone heights of 2, 2.25 and 2.5 meters, respectively. For a tungsten zone height of 2 and 2.25 meters, the atomic displacement rate at ~2.2 meters above the midplane is about two and one order of magnitude higher than

*This is the total energy deposited in the inner magnet, i.e., the portion of the magnet close to the toroidal axis. For the heat load deposited in the whole magnet, another ~50 watts is to be added to the above.

that at the midplane, respectively. The maximum resistivity change occurring in these designs would be correspondingly ~40 and 2 times that of the unirradiated resistivity after one year of operation. However, for the 2.5 meter tungsten zone height design, the atomic displacement at the magnet region above midplane is always less than that at midplane. The maximum resistivity change is only ~25% for one year of irradiation. These effects can be easily seen in Fig. 11 where contours of the atomic displacement rates are depicted for designs with 2.25 and 2.5 meters high tungsten zones. If the parameter value at midplane is designed to be an optimum then the values for the region above midplane would not be acceptable in the 2.5 m design. Hence a tungsten zone height of no less than 2.5 meters seems to be unavoidable in the NUWMAK design. The situation for dose rate and neutron fluence are similar to that for atomic displacement considerations.

V. Final Results for NUWMAK Blanket and Shield Design

In the following, computational results for the final NUWMAK blanket and shield, which evolved from the parametric survey studies in previous sections, will be presented. In this final design model, the 20 cm Li_{62} Pb_{38} blanket will be followed by a 35 cm tungsten zone, a 45 cm boron carbide zone and a 5 cm lead zone. The tungsten zone height is designed to be 2.5 meters. The specific composition and dimensions for each zone are tabulated in Table IV. (The zone thicknesses given here are those at the midplane). Natural lithium is employed in the Li_{62} Pb_{38} eutectic.

V.A. Tritium Breeding, Neutron Multiplication and Nuclear Heating

In Table V are shown the tritium breeding, neutron multiplication and nuclear heating for the final blanket and shield design. The tritium breeding ratio for this system is 1.54 tritons per D-T neutron, of which about 90% is from $^{6}Li(n,\alpha)$ reactions. The tritium breeding from the outer blanket alone is about 1.24 tritons per D-T neutron which is already more than is required in the design goal described in Sec. II. As discussed in Ref. 1 and 6, the placing of Li_{62} Pb_{38} eutectic in the inner blanket is primarily due to the internal energy storage requirement to minimize the thermal cycling of the structure and coolant output temperature.

The neutron multiplication in this system which is dominated by Pb(n,2n) reactions is ~0.57 neutrons per D-T neutron as shown in this table. The total nuclear heating in the blanket/shield system is ~17.15 MeV per D-T neutron, of which ~35% is contributed by gamma-ray heating.

Note that the gamma-ray heating itself is more than 50% as far as the nuclear heating in the inner blanket/shield is concerned. This can be attributed to the contribution of the nuclear heating in the tungsten zone (zone 4) as shown in Table VII. It is 1.22 MeV per D-T neutron, most of which is from gamma-ray heating reflecting the fact that the Q values for $W(n,\gamma)$ reactions are on average ~6 MeV, which is higher than for $^{6}Li(n,\alpha)$ reactions, ~4.8 MeV. In Table VI, the nuclear heating in the structure and coolant is shown to be 2.14 MeV per D-T neutron, which is ~12% of the total. The energy deposition in the coolant alone is ~8% of the total. The recoverable energy for this system can be collected from the total energy deposited in the blanket/shield zone shown in Table VII excluding zones 2, 3 and 14. Hence, the total recoverable energy is found to be more than 99% of the total. The total thermal output (including alpha heating) for the NUWMAK blanket/shield is thus 2292 MW during the burn. The net electrical output is 660 MW, if a duty factor of 0.91 and a net efficiency of 31.5% are assumed. The spatial nuclear heating rates in the inner as well as outer blanket/shield at the midplane are shown in Fig. 12.

V.B. Radiation Damage of Superconducting Magnet

The maximum atomic displacement rate in the aluminum stabilizer, neutron fluence in the superconductors, and dose rate in the superinsulators for NUWMAK are given in Table VIII, and are 2×10^{-6} dpa/year, 7×10^{15} n/cm^2 per year and 3×10^{7} rads/year, respectively. The corresponding magnet operation parameters after one year of continuous operation are as follows. The resistivity change in the aluminum stabilizer is found to be less

than 25%, the critical current density change in the NbTi conductors is less than 0.5%. The most crucial design consideration is that after two years of continuous operation, the resistivity change will reach the design limit as discussed in Sec. II. In fact, this is designed to be consistent with the blanket lifetime.[19] Hence, the plant will be shut down, the magnet annealed and the blanket replaced after every two years of operation.

For the integrity and thermal insulation properties of the superinsulation materials, after 30 years of continuous operation, which is about the plant lifetime, the dose in the superinsulator will be $\sim 1 \times 10^9$ rads. Under such a dose, mylar based superinsulators would experience severe radiation damage while the epoxy based superinsulators only show incipient to mild damage. Hence, epoxy based superinsulators must be used in regions where intense radiation dose occurs.

The spatial atomic displacement, neutron fluence and dose rate in the magnet are shown in Figs. 13 and 14. The spatial nuclear heating rate as well as the gas production rates are also depicted in Fig. 15.

VI. Radioactivity

The calculation of activity and related quantities in NUWMAK have been performed using the techniques developed for use in previous studies.[2,3,4] Specifically the code DKR[20] was used to calculate specific activities using the flux spectrum from the neutronics calculations and nuclear data from the DCDLIB[21] code. As in previous calculations the energy from decay gammas is assumed to be deposited at the site of the decay unless gamma transport calculations are to be performed to obtain shielding information.

The calculations in previous studies were for the most part performed on a one-dimensional basis, i.e. the neutron flux and blanket materials were assumed to be independent of the poloidal angle. In NUWMAK, however, because of the heterogeneous nature of the blanket, involving several regions with different materials, and the two-dimensional shape of the plasma, an attempt was made to make the calculations reflect these effects more realistically than in the past.

A schematic of the NUWMAK blanket as considered for the radioactivity calculations is shown in Fig. 16. The composition of the various regions is given in Table IV. As discussed in previous sections of this report, the inner regions of the blanket (zones A-C) are mainly shields to reduce the radiation and heat loads on the magnets and associated components. For the activity calculations to be performed with the same detail as the flux calculations a DKR calculation would have to be made at each mesh point

resulting in some 1600 calculations which would then have to be properly volume weighted and processed together. This course of action was not taken for two reasons. First, the amount of effort required was deemed to be too large and second, at this stage of the study it was judged that such detailed calculations were not necessary to determine the activity of the design adequately for comparison with other results and to evaluate the effects of the radioactive decay. Consequently, calculations were made only along those traverses shown in Fig. 16. Further simplification was obtained by breaking the various regions along the traverses into subregions using an average flux in each of these regions. This procedure was also used in previous one-dimensional studies. The specific activities calculated along each of these traverses was then taken to be representative of the average activity in an associated zone so that with proper volume weighting the total activity of a zone or combination of zones could be found. Since the highest specific activity occurs in the first wall additional calculations were made at additional first wall points around the plasma cavity.

VI-A. Radioactivity, Afterheat and BHP

The results of the calculations are shown in Figs. 17-19. Fig. 17 shows the radioactivity of the reactor in curies per watt thermal. For comparison purposes the activity of UWMAK-I is also shown. The activity changes very little during the time immediately after shutdown being almost

constant for the first month or so. This means that very little relief in activity levels around the reactor can be obtained by using a waiting period after shutdown. However, since the dose rates occurring outside of the shield are primarily the result of gammas emitted near the edge of the shield, it does not necessarily follow that the dose rates in that region will follow this same pattern. This will be discussed in the next subsection. From the point of view of intermediate term activity the curves show that after about 10 years the activity levels are down by between 4-5 orders of magnitude. It may be also noted that most of the activity originates in the inner region of the blanket.

In comparing the activity with the stainless steel UWMAK-I design it is seen that some improvement has been made especially in the one year to 1000 year time span. Initially the activity per watt is only lower by a factor of about two. The afterheat results (Fig. 18) and BHP results (Fig. 19) show qualitatively similar behavior with the primary difference being the very long term behavior of the BHP for NUWMAK.

As seen in Fig. 19, it would appear that at very long times the biological hazard potential (BHP) of NUWMAK is significantly higher than the BHP of a stainless steel system such as UWMAK-I. This would imply a long term radioactivity problem in any machine with a Pb-Li blanket with all its attendant difficulties and problems. It is unlikely that this is the case. In calculating the BHP the allowable concentrations used are taken from chapter 10 part 20 of the Code of Federal Regulations. In the case of ^{205}Pb no limits are given and therefore the default value of 10×10^{-10} $\mu Ci/ml$ is

used. However, ^{205}Pb decays by electron capture to the ground state of ^{205}Tl. Furthermore, the Q value for this reaction is so low that the electron captured is from the L shell. Consequently, the X-rays emitted following a transition are of low energy viz. ~ 11 keV. It would seem then that ^{205}Pb should be no worse than ^{203}Pb which has an allowable concentration of 6×10^{-8} μCi/ml and likely would be significantly less of a problem. Even raising the allowable concentration by a factor of 20 means that at these very long times it is the ^{26}Al activity that would dominate.

VI-B. Dose Rate After Shutdown

The gamma dose rate following shutdown has been calculated at two positions, the center of the plasma region and the outside of the shield at the mid-plane of the outer blanket. The calculation of the latter presented more difficulty since neutronics calculations were made only out to a major radius of 7.25 m and thus it was not possible to determine decay gamma sources beyond this point. In an attempt to obtain an estimate of the dose outside the shield it was assumed the shield would be extended to a thickness of 85 cm thus ending the shield at a major radius of 7.95 m. In this extended region of the shield the decay gamma source was taken to be a constant with the same strength as in the outermost region of the neutronics calculation, i.e. at 7.25 m. As the decay gamma source is expected to drop off between 7.25 and 7.95 m, this calculation should overestimate the dose outside the shield. The results of the calculations are shown in Table IX. As

anticipated, the radiation levels inside the torus are quite high being about 7.5×10^5 rem/hr at shutdown. The reduction in level with time is quite slow requiring about one month to be reduced by a factor of ten and about one year for a factor of 100. Even after ten years the predicted dose level is still about 3 rem/hr.

It is interesting to note the effects the selection of materials has on the contribution to the dose rate. For example, the activity levels of the inner and outer blankets are about the same. However, the inner blanket contributes much less to the dose rate inside the torus. This is because of the presence of tungsten in the inner region which provides a substantial amount of self shielding. Consequently, the contribution of the inner blanket to the dose rate is about two orders of magnitude less than that of the outer blanket.

The situation outside the shield appears to be rather favorable. The predicted dose rates are low even at shutdown being ~ 60 mrem/hr and dropping in one hour to 6.1 mrem/hr, and to 2.6 mrem/hr after one day. However, this result should be viewed with some caution even though the gamma decay source has been overestimated in the outer shield region. The dose rate outside the shield is determined to a large degree by the activity in the outer region of the shield if the shield is assumed to completely cover the blanket. Variations in structure in this region can alter the predicted dose rate considerably. In addition, streaming problems due to the necessity of penetrations in the blanket and shield less carefully attended to could raise the dose levels significantly.

Nevertheless, it appears that with care the post shutdown dose rates can be low enough to consider hands on shift maintenance, if not immediately after shutdown, within a relatively short time.

VII. Conclusions

The nucleonic design of the blanket and shield for a high power density, compact, boiling water cooled tokamak fusion reactor, NUWMAK, has been completed. The calculational analysis and conclusions may be summarized as follows.

1. A tritium breeding ratio of 1.54 tritons per D-T neutron is obtained. More than 90% of the breeding is contributed from $^{6}Li(n,\alpha)T$ reactions. The outer breeding blanket alone contributes 1.24 tritons per D-T neutron which is more than adequate.
2. There is no incentive to employ enriched lithium in the $Li_{62}\ Pb_{38}$ eutectic.
3. The total recoverable nuclear heat deposited in the blanket and shield is 17.15 MeV per D-T neutron, of which ~35% comes from gamma-ray heating. This amount of heat represents more than 99% of the total energy output in the system.
4. The total thermal power output is 2292 MW. The net electric output is 660 MW if a duty factor of 0.91 and a net efficiency of 31.5% are considered.
5. The atomic displacement in the aluminum stabilizer is $\sim 4 \times 10^{-6}$ dpa after two years of continuous operation. The corresponding resistivity change is ~50%. While the neutron fluence at the superconductor is $\sim 1.4 \times 10^{16}$ n/cm^2, the reduction of its critical current density is no more than 1%.

6. With the dose of ~ 1 x 10^9 rads after 30 years of operation, the only endurable organic superinsulator is an epoxy-base superinsulator. The mylar-base superinsulator will be excluded in the most severely damaged regions.
7. The radioactivity, afterheat and biological hazard potential after one year of continuous operation are 0.8 curie/W_{th}, 0.5% of operating power and 2 x 10^2 km^3 air/kW_{th}, respectively. However, they drop by between 4-5 orders of magnitude 10 years after shutdown.
8. The post shutdown dose rates outside the regular outer shield are favorable to hands on shift maintenance. They drop to less than 2.6 mrem/hr one day after shutdown.

References

1. R. W. Conn et al., "NUWMAK: An Attractive Medium Field, Medium Size, Conceptual Tokamak Reactor", Proc. of Third Topical Meeting on the Technology of Controlled Thermonuclear Fusion, American Nuclear Society, Santa Fe, New Mexico, 9-11 May 1978.

2. B. Badger et al., "UWMAK-I, A Wisconsin Toroidal Fusion Reactor Design", Fusion Research Program Report UWFDM-68, University of Wisconsin (1973).

3. B. Badger et al., "UWMAK-II, A Conceptual Tokamak Power Reactor Design", Fusion Research Program Report UWFDM-112, University of Wisconsin (1975), See also Nucl Engr. and Design, 39, 5 (1976).

4. B. Badger et al., "UWMAK-III, A High Performance Noncircular Tokamak Power Reactor Design", Electric Power Research Institute Report ER-368, EPRI (1976).

5. I. N. Sviatoslavsky, "Engineering Design Considerations for Facilitating Maintainability of Fusion Reactors", Proc. of Third Topical Meeting on the Technology of Controlled Thermonuclear Fusion, American Nuclear Society, Santa Fe, New Mexico, 9-11 May 1978.

6. D. K. Sze et al., "A BWTR (Boiling Water Tokamak Reactor) Blanket Study", ibid.

7. W. F. Vogelsang, "Breeding Ratio, Inventory, and Doubling Time in a D-T Fusion Reactor", Nuclear Technology 15, 470 (1972).

8. M. A. Abdou and R. W. Conn, "A Comparative Study of Several Fusion Reactor Blanket Studies", Nucl. Sci. Eng. 55, 256 (1974).

9. M. A. Abdou, "Radiation Considerations for Superconducting Fusion Magnets", ANL/FPP/TM-92, Argonne National Laboratory report. (1977)

10. G. M. McCracken and S. Blow, "The Shielding of Superconducting Magnets in a Fusion Reactor", CLM-R120, Culham Laboratory (1972).

11. C. A. M. Van der Klein, "The Organic Insulation in Fusion Reactor Magnet Systems", RCN-240, Reactor Centrum Nederland (1975).

12. R. D. Hay, "Superconducting Magnetic Electrical Insulations", Proc. of the Meeting on CTR Electrical Insulators, May 17-19, 1976, LASL, CONF-760558 (Feb. 1978), p. 65.

13. W. W. Engle, Jr., "A User's Manual for ANISN", K-1693, Oak Ridge Gaseous Diffusion Plant (1967).

14. F. R. Mynatt et al., "The DOT-III Two-Dimensional Discrete Ordinates Transport Code", Oak Ridge National Laboratory, ORNL-TM-4280 (1973).

15. D. M. Plaster et al., "Coupled 100 Group Neutron and 21 Gamma-Ray Cross Sections for EPR Calculations", ORNL-TM-4873, Oak Ridge National Laboratory (1975).

16. T. A. Gabriel et al., "Radiation Damage Calculations: Primary Knock-On Atom Spectra, Displacement Rates, and Gas Production Rates", Nucl. Sci. Eng. 61, 21 (1976).

17. M. A. Abdou and C. W. Maynard, "Nuclear Design of the Magnet Shield for Fusion Reactors", Proc. First Topical Meeting Technology of Controlled Nuclear Fusion, CONF-740402-R1, Vol. I, p. 685, U. S. Atomic Energy Commission (1974).

18. M. A. Abdou, "Nuclear Design of Blanket/Shield System for a Tokamak Experimental Power Reactor", Nuclear Technology 29, 7 (1976).

19. The blanket lifetime for NUWMAK is estimated ~10 MW-Yr/m^2, and is ~2 years of continuous operation. Private communications with R. W. Conn and G. L. Kulcinski.

20. T. Y. Sung and W. F. Vogelsang, "DKR: A Radioactivity Calculation Code for Fusion Reactors", UWFDM-170, Nuclear Engineering Department, University of Wisconsin (Sept 1976).

21. T. Y. Sung and W. F. Vogelsang, "Decay Chain Data Library for Radioactivity Calculations", UWFDM-171, Nuclear Engineering Department, University of Wisconsin (Sept 1976).

List of Tables

Table I

Major Features of NUWMAK Design

Power	
Total Thermal Power	2097 MW_t
Net Electric Power	660 MW_e
Plasma	
Major Radius	5.13 m
Minor Radius	1.13 m
Plasma Height to Width Ratio (b/a)	1.64
Plasma Current	7.2 MA
Toroidal Beta	6%
$n_e\tau_E$	2×10^{14} cm^{-3}-sec
q(a)	2.64
Magnet	
On-Axis Toroidal Field	6.05 Tesla
Toroidal Field at NbTi Conductor	11.5 Tesla
Stabilizer	Aluminum
Number of Toroidal Field Coils	8
Number of Cu Trim Coils	16
Blanket	
Structural Material	Titanium Alloy
Coolant	Boiling Water
Breeding Material	$Li_{62}Pb_{38}$
Average Neutron Wall Loading	4.34 MW/m^2

Table II

Neutron 25 Energy Group Structure in eV

Group Limits

Group	E(Top)	E(Low)	E(Mid Point)	Corresponding Fine Groups in 100 Group Structure[a]
1	1.4918 (+7)	1.3499 (+7)	1.4208 (+7)	1
2	1.3499 (+7)	1.2214 (+7)	1.2856 (+7)	2
3	1.2214 (+7)	1.1052 (+7)	1.1633 (+7)	3
4	1.1052 (+7)	1.0000 (+7)	1.0526 (+7)	4
5	1.0000 (+7)	9.0484 (+6)	9.5242 (+6)	5
6	9.0484 (+6)	8.1873 (+6)	8.6178 (+6)	6
7	8.1873 (+6)	7.4082 (+6)	7.7979 (+6)	7
8	7.4082 (+6)	6.7032 (+6)	7.0557 (+6)	8
9	6.7032 (+6)	6.0653 (+6)	6.3843 (+6)	9
10	6.0653 (+6)	5.4881 (+6)	5.7787 (+6)	10
11	5.4881 (+6)	4.4933 (+6)	4.9907 (+6)	11 - 12
12	4.4933 (+6)	3.6788 (+6)	4.0860 (+6)	13 - 14
13	3.6788 (+6)	3.0119 (+6)	3.3453 (+6)	15 - 16
14	3.0119 (+6)	2.4660 (+6)	2.7390 (+6)	17 - 18
15	2.4660 (+6)	1.3534 (+6)	1.9097 (+6)	19 - 24
16	1.3534 (+6)	7.4274 (+5)	1.0481 (+6)	25 - 30
17	7.4274 (+5)	4.0762 (+5)	5.7518 (+5)	31 - 36
18	4.0762 (+5)	1.6573 (+5)	2.8667 (+5)	37 - 45
19	1.6573 (+5)	3.1828 (+4)	9.8779 (+4)	46 - 54
20	3.1828 (+4)	3.3546 (+3)	1.7591 (+4)	55 - 63
21	3.3546 (+3)	3.5358 (+2)	1.8541 (+3)	64 - 72
22	3.5358 (+2)	3.7267 (+1)	1.9542 (+2)	73 - 81
23	3.7267 (+1)	3.9279 (+0)	2.0597 (+1)	82 - 90
24	3.9279 (+0)	4.1399 (-1)	2.1718 (+0)	91 - 99
25	4.1399 (-1)	2.200 (-2)	2.1800 (-1)	100

a. the original EPR library group structure

Table III

Solid and Liquid Densities of Pb, Li and Their Alloys

Material	Solid Density-g/cm^3	Liquid Density at 500°C-g/cm^3
Pb	11.34(a)	10.45(b)
PbLi	8.1(c)	6.31(d)
$Pb_{38}Li_{62}$-eutectic	6.5(e)	5.01(d)
Li_5Pb_2	5.33(c)	4.04(d)
Li	0.534(a)	0.485(b)

(a) From CRC Handbook of Chemistry and Physics, 56th Ed. pp. B-104, 107.

(b) For Pb

$$\rho Pb = 10.71 - 0.00139\ (t-327) \qquad 327°C < t < 800°C$$

For Li

$$\rho Li = 0.515 - 1.01 \times 10^{-4}\ (t-200) \qquad 200°C < t < 1600°C$$

These formulas giving the liquid metal density as a function of temperature are from p. B-240 of CRC Handbook of Chem. and Phys.

(c) From Gmelins Handbuch Der Anorganischen Chemie, Blei: Teil C3, #47, page 982.

(d) Calculated assuming ideal solution of Pb and Li.

(e) Interpolated between the experimental values of 8.1 for PbLi and 5.33 for Li_5Pb_2.

Table IV

Material Compositions for the NUWMAK Blanket and Shield Neutronics Model at Midplane

Specification	Zone Number	Thickness (meter)	Composition (All percentage by Volume)
Magnet	1	0.30	80% Al + 12.8% Epoxy + 7.2% He (liquid)
Lead Shield	2	0.10	4% Ti Alloy + 2% H_2O + 1% Pb + 93% Pb[a]
B_4C Shield	3	0.40	4% Ti Alloy + 2% H_2O + 1% Pb + 93% B_4C[b]
Tungsten Shield	4	0.35	4% Ti Alloy + 2% H_2O[c] + 1% Pb + 93% W[d]
Inner Breeding Blanket	5 (B-2)	0.10	6% Ti Alloy + 3.9% H_2O[e] + 1.0% Pb + 89.1% Li_{62} Pb_{38}[f]
	6 (B-1)	0.10	9.6% Ti Alloy + 8.6% H_2O[e] + 2.4% Pb + 79.4% Li_{62} Pb_{38}[f]
Plasma and Vacuum	7	0.05	Vacuum
	8	2.25	Plasma
	9	0.15	Vacuum
Outer Breeding Blanket	10 (B-1)	0.10	9.6% Ti Alloy + 8.6% H_2O[e] + 2.4% Pb + 79.4% Li_{62} Pb_{38}[f]
	11 (B-2)	0.15	6% Ti Alloy + 3.9% H_2O[e] + 1.0% Pb + 89.1% Li_{62} Pb_{38}[f]
	12 (B-3)	0.25	3.8% Ti Alloy + 1.8% H_2O[e] + 0.3% Pb + 94.1% Li_{62} Pb_{38}[f]
Graphite Reflector	13	0.20	3.5% Ti Alloy + 1% H_2O[e] + 0.25% Pb + 95.25% Graphite
B_4C Shield	14	0.20	3.5% Ti Alloy + 1% H_2O + 0.25% Pb + 95.25% B_4C[b]

a. 90% dense b. 95% dense c. average density factor is 94% d. 90% dense e. average density factor 90% f. average density between solid and liquid phases is 5.75 g/cc

Table V

Tritium Breeding, Neutron Multiplication and Nuclear Heating in NUWMAK

Tritium Production (T/D-T Neutron)	INNER	OUTER	TOTAL
$^{6}Li(n,\alpha)$ (T_6)	0.2604	1.1249	1.3853
$^{7}Li(n,n'\alpha)$ (T_7)	0.0375	0.1192	0.1567
$T_6 + T_7$	0.2979	1.2441	1.5420
Neutron Multiplication (Reaction/D-T Neutron)	**INNER**	**OUTER**	**TOTAL**
Pb(n,2n)	0.1339	0.4181	0.5520
W(n,2n)	0.0137	------	0.0137
Total	0.1476	0.4181	0.5657
Nuclear Heating (MeV/D-T Neutron)	**INNER**	**OUTER**	**TOTAL**
Neutron	2.2665	8.9298	11.1963
Gamma-Ray	2.4143	3.5422	5.9565
Neutron + Gamma-Ray	4.6808	12.4720	17.1528

Table VI

Nuclear Heatings by Zone in the Structure/Piping and Coolant in NUWMAK (in units of MeV per D-T neutron)

Zone Number	Ti	Al	V	Pb	H	O	Subtotal
2	1.48(-7)	5.33(-9)	6.98(-9)	1.64(-7)	7.88(-9)	1.54(-8)	3.47(-7)
3	1.26(-4)	4.46(-6)	6.00(-6)	1.30(-4)	1.22(-5)	7.64(-6)	2.80(-4)
4	9.46(-3)	4.82(-4)	4.52(-4)	9.00(-3)	1.28(-2)	1.89(-3)	3.41(-2)
5	1.64(-2)	1.34(-3)	7.65(-4)	3.57(-3)	5.32(-2)	7.30(-3)	8.26(-2)
6	7.97(-2)	7.22(-3)	3.38(-3)	2.35(-2)	2.56(-1)	4.90(-2)	4.19(-1)
10	2.44(-1)	2.19(-2)	1.04(-2)	7.27(-2)	7.95(-1)	1.49(-1)	1.29
11	4.52(-2)	3.93(-3)	2.17(-3)	8.98(-3)	1.71(-1)	2.22(-2)	2.53(-1)
12	7.52(-3)	6.49(-4)	4.39(-4)	6.64(-4)	3.34(-2)	3.14(-3)	4.58(-2)
13	5.09(-3)	2.14(-4)	5.50(-4)	2.60(-3)	2.09(-3)	3.84(-4)	1.09(-2)
14	1.91(-3)	6.58(-5)	9.06(-5)	1.95(-3)	1.15(-4)	1.10(-4)	4.24(-3)
Sum	4.09(-1)	3.58(-2)	1.82(-2)	1.23(-1)	1.32	2.33(-1)	2.14

Table VII

Nuclear Heatings by Zone in Breeding and Shield Materials
in NUWMAK (in units of MeV per D-T neutron)

Zone Number	W	Pb	^{6}Li	^{7}Li	^{10}B	^{11}B	C	Subtotal	Total[a]
2	-----	1.527(-5)	-----	-----	-----	-----	-----	1.527(-5)	1.562(-5)
3	-----	-----	-----	-----	4.689(-3)	9.793(-4)	4.482(-5)	5.713(-3)	5.993(-3)
4	1.2209	-----	-----	-----	-----	-----	-----	1.2209	1.2550
5	-----	0.3179	0.4299	0.1388	-----	-----	-----	0.8866	0.9692
6	-----	0.7769	0.8769	0.3776	-----	-----	-----	2.0314	2.4504
10	-----	2.4046	2.8440	1.1549	-----	-----	-----	6.4035	7.6935
11	-----	0.8000	1.7221	0.4328	-----	-----	-----	2.9549	3.2079
12	-----	0.2082	1.0250	0.1337	-----	-----	-----	1.3669	1.4127
13	-----	-----	-----	-----	-----	-----	0.0752	0.0752	0.0861
14	-----	-----	-----	-----	4.936(-2)	1.370(-2)	5.064(-3)	0.0681	0.0724
Sum	1.2209	4.5076	6.8979	2.2378	0.0540	0.0147	0.0803	15.013	17.153

a. includes heatings in the structure/piping and coolant shown in Table VI.

Table VIII

Radiation Damage Parameters for the Superconducting Magnet in NUWMAK

Maximum Atomic Displacement Rate in the Aluminum Stabilizer (dpa/year)	2×10^{-6}
Maximum Dose Rate in the Epoxy-Base Superinsulators (rad/year)	3×10^{7}
Maximum Neutron Flux in the NbTi Superconductors (n/cm^2/year)	7×10^{15}
Total Nuclear Heatings in TF Coils (Watts)	$\sim$ 500

Table IX

Calculated Dose Rates in NUWMAK for Times After Shutdown

Position: Inside Torus

Time After Shutdown	From Inner Blanket (mRem/hr)	From Outer Blanket (mRem/hr)	Total (mRem/hr)
0	3.37 + 06	7.46 + 08	7.49 + 08
1 Min	3.28 + 06	6.16 + 08	6.19 + 08
1 Hr	2.92 + 06	5.66 + 08	5.69 + 08
1 Da	1.79 + 06	3.85 + 08	3.87 + 08
1 Mo	2.90 + 05	7.56 + 07	7.59 + 07
1 Yr	1.93 + 04	5.43 + 06	5.45 + 06
10 Yr	1.02 + 00	3.31 + 03	3.32 + 03
100 Yr	8.31 - 02	1.35 + 02	1.36 + 02
1000 Yr	7.42 - 02	8.35 + 01	8.36 + 01
10 kYr	6.19 - 02	1.96 + 01	1.97 + 01
100 kYr	5.62 - 02	1.59 + 01	1.60 + 01
1 MYr	2.49 - 02	9.80 + 00	9.82 + 00

Position: Outside Shield

Time After Shutdown	Dose Rate (mRem/hr)
0	6.08 + 01
1 Min	2.51 + 01
1 Hr	6.10 + 00
1 Da	2.62 + 00
1 Mo	2.18 - 01
1 Yr	1.44 - 02
10 Yr	2.91 - 06
100 Yr	2.74 - 07
1000 Yr	2.51 - 07
10 kYr	1.18 - 07
100 kYr	4.70 - 08
1 MYr	2.36 - 08

List of Figures

FIGURE 1

CROSS-SECTIONAL VIEW OF NUWMAK

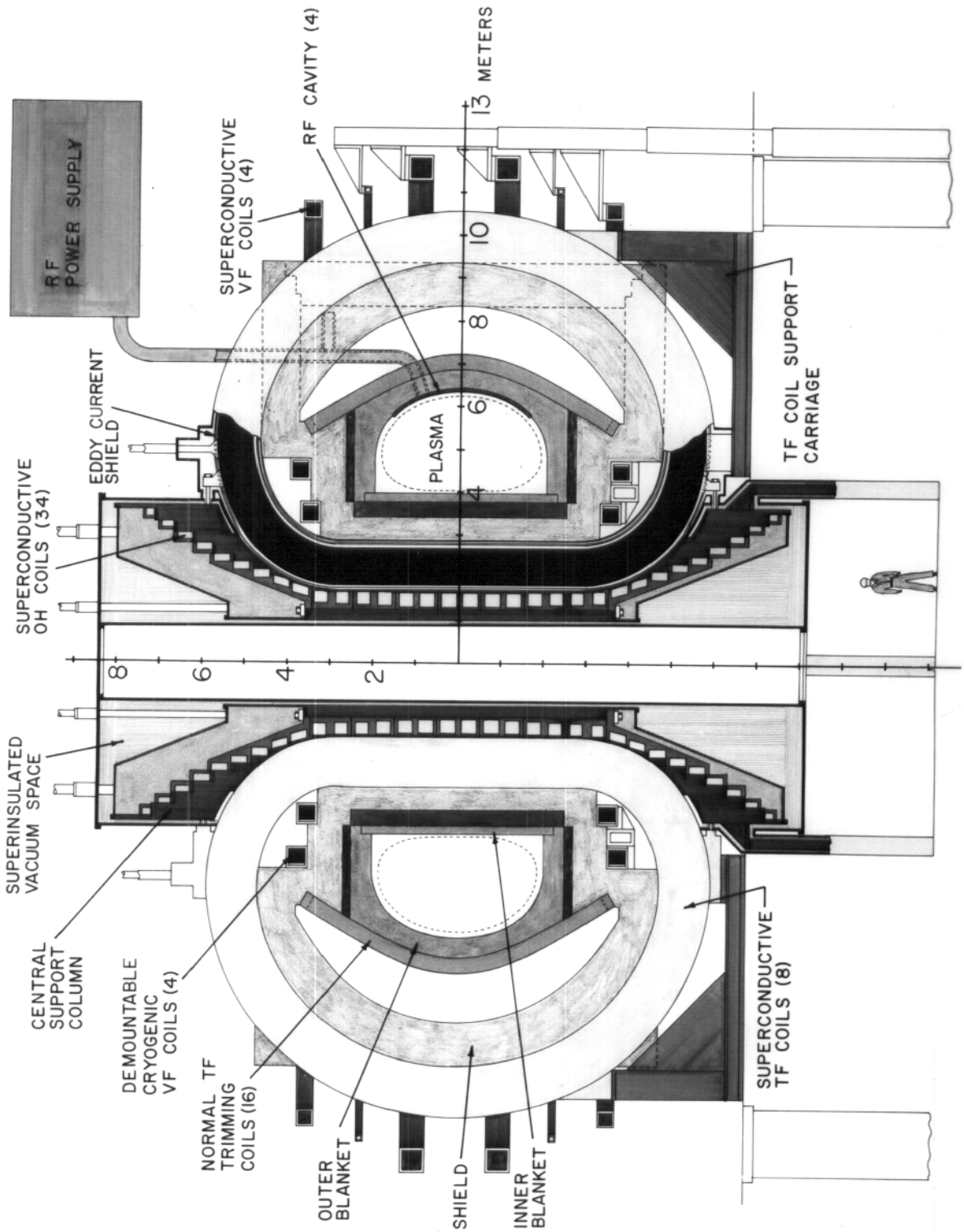

FIGURE 2

SCHEMATIC OF THE BLANKET AND SHIELD FOR NUWMAK

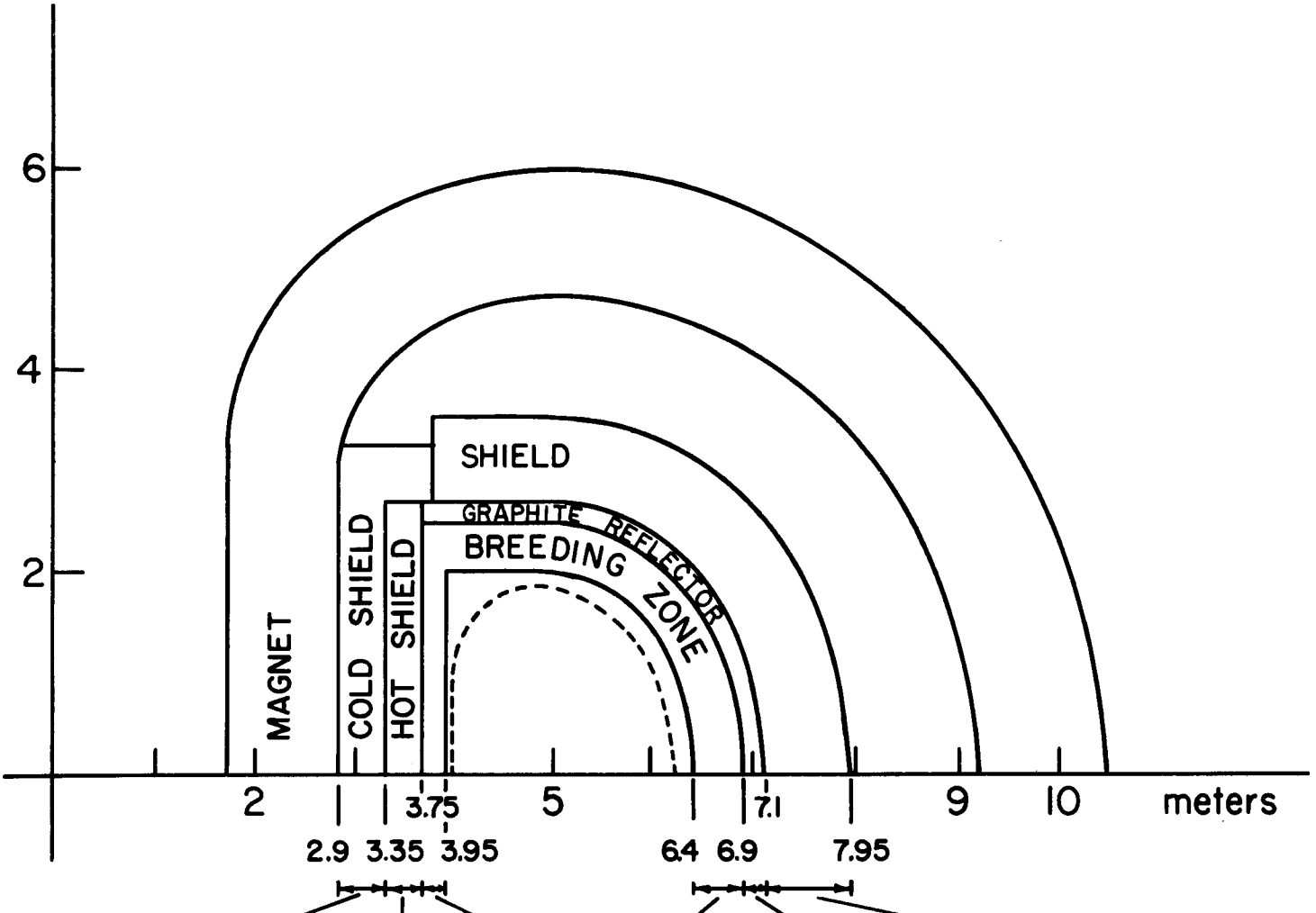

COLD SHIELD	HOT SHIELD	BREEDING ZONE	GRAPHITE REFLECTOR	SHIELD
3.5% Ti alloy	4% Ti alloy	5.7% Ti alloy	3.5% Ti alloy	3.5% Ti alloy
95.25% B_4C	93% W	89.4% Pb Li	95.25% C	95.25% B_4C
1% H_2O	2% H_2O	3.7% H_2O	1% H_2O	1% H_2O
0.25% Pb	1% Pb	1.2% Pb	0.25% Pb	0.25% Pb

FIGURE 3

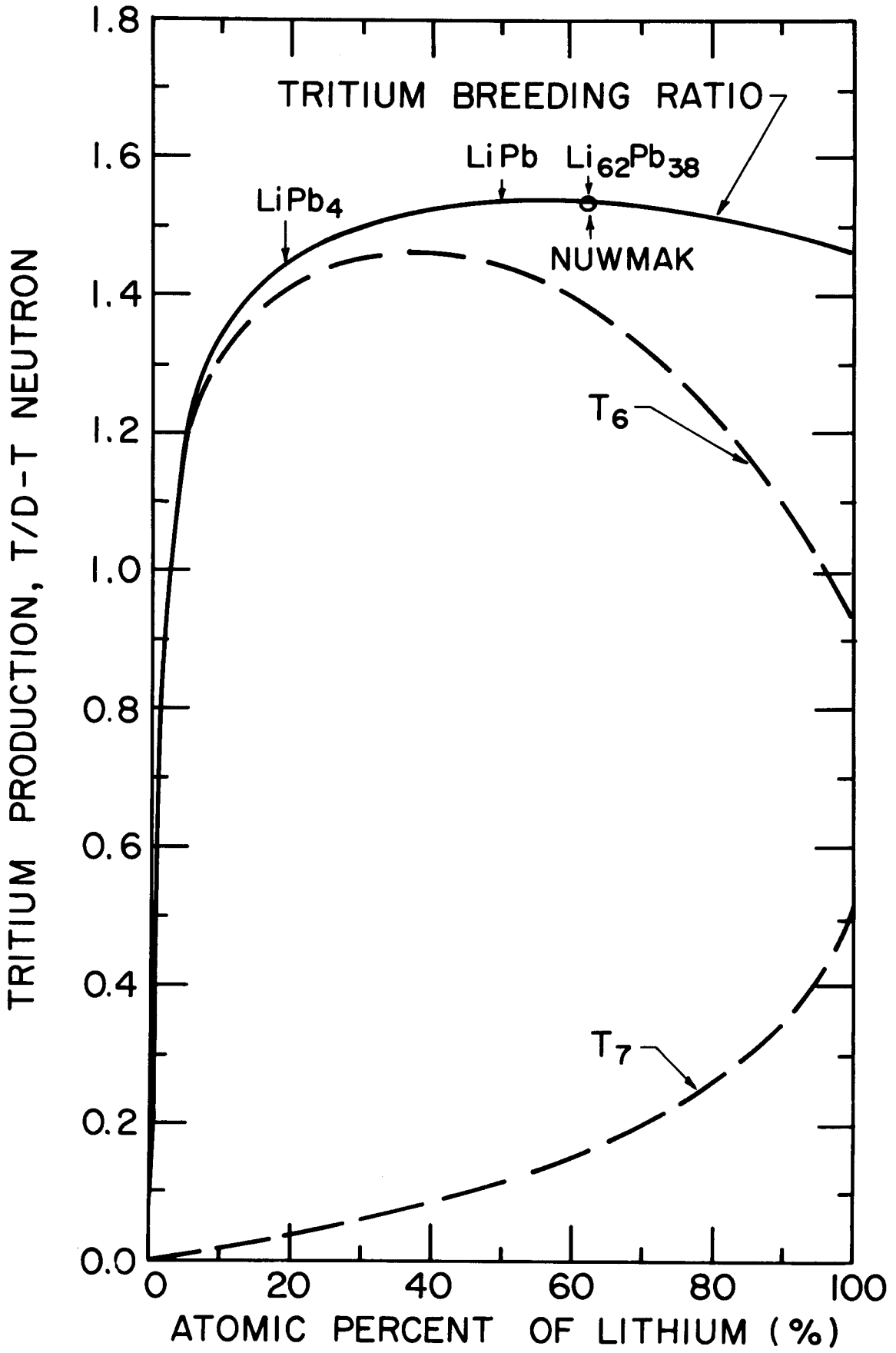
TRITIUM BREEDING RATIO
LiPb
Li62Pb38
LiPb4
NUWMAK
T6
T7
TRITIUM PRODUCTION, T/D-T NEUTRON
ATOMIC PERCENT OF LITHIUM (%)
1.8
1.6
1.4
1.2
1.0
0.8
0.6
0.4
0.2
0.0
0
20
40
60
80
100

FIGURE 4

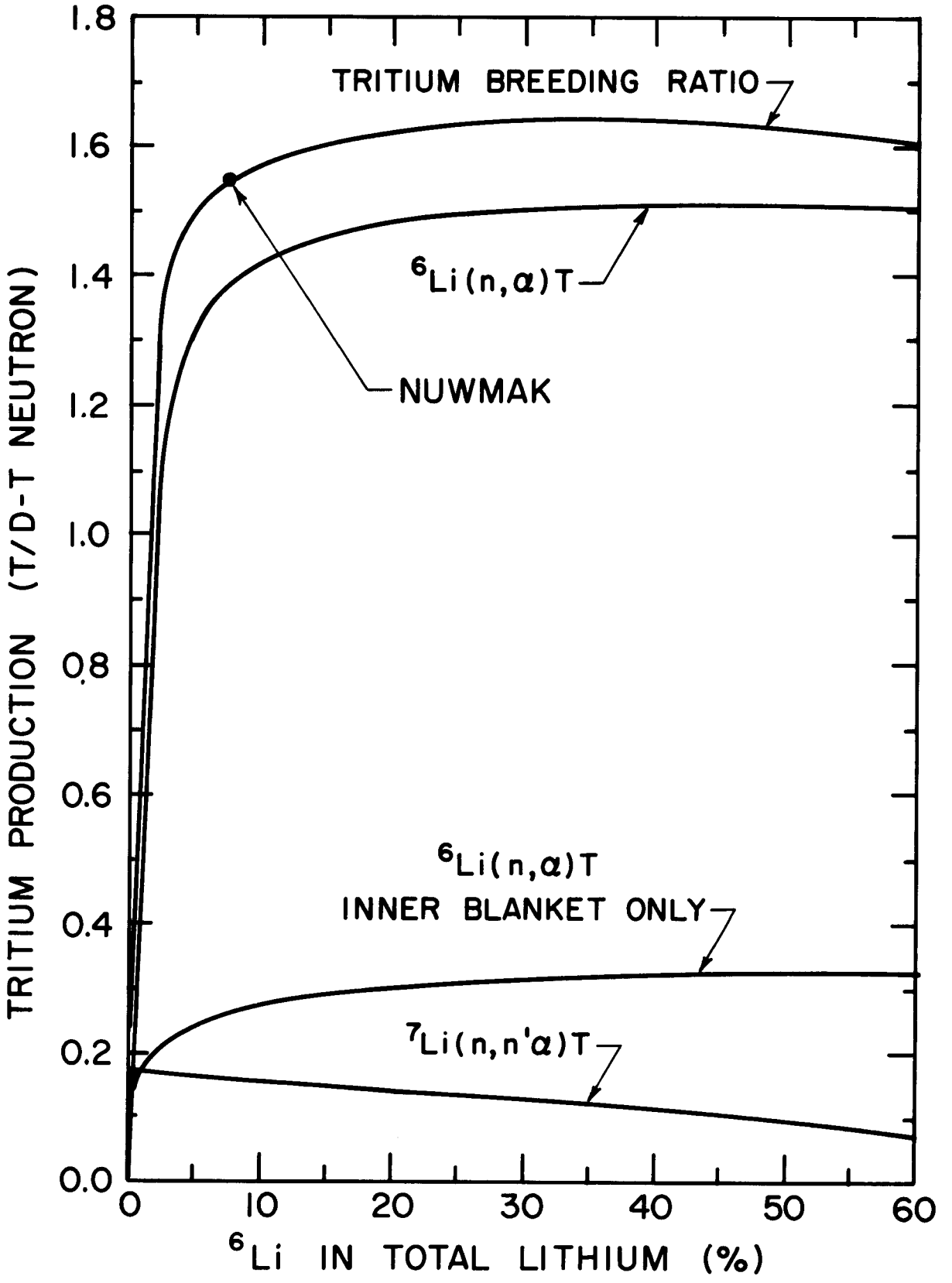
TRITIUM BREEDING RATIO
$^{6}Li(n,\alpha)T$
NUWMAK
$^{6}Li(n,\alpha)T$
INNER BLANKET ONLY
$^{7}Li(n,n'\alpha)T$
TRITIUM PRODUCTION (T/D-T NEUTRON)
^{6}Li IN TOTAL LITHIUM (%)
0.0
0.2
0.4
0.6
0.8
1.0
1.2
1.4
1.6
1.8
0
10
20
30
40
50
60

FIGURE 5

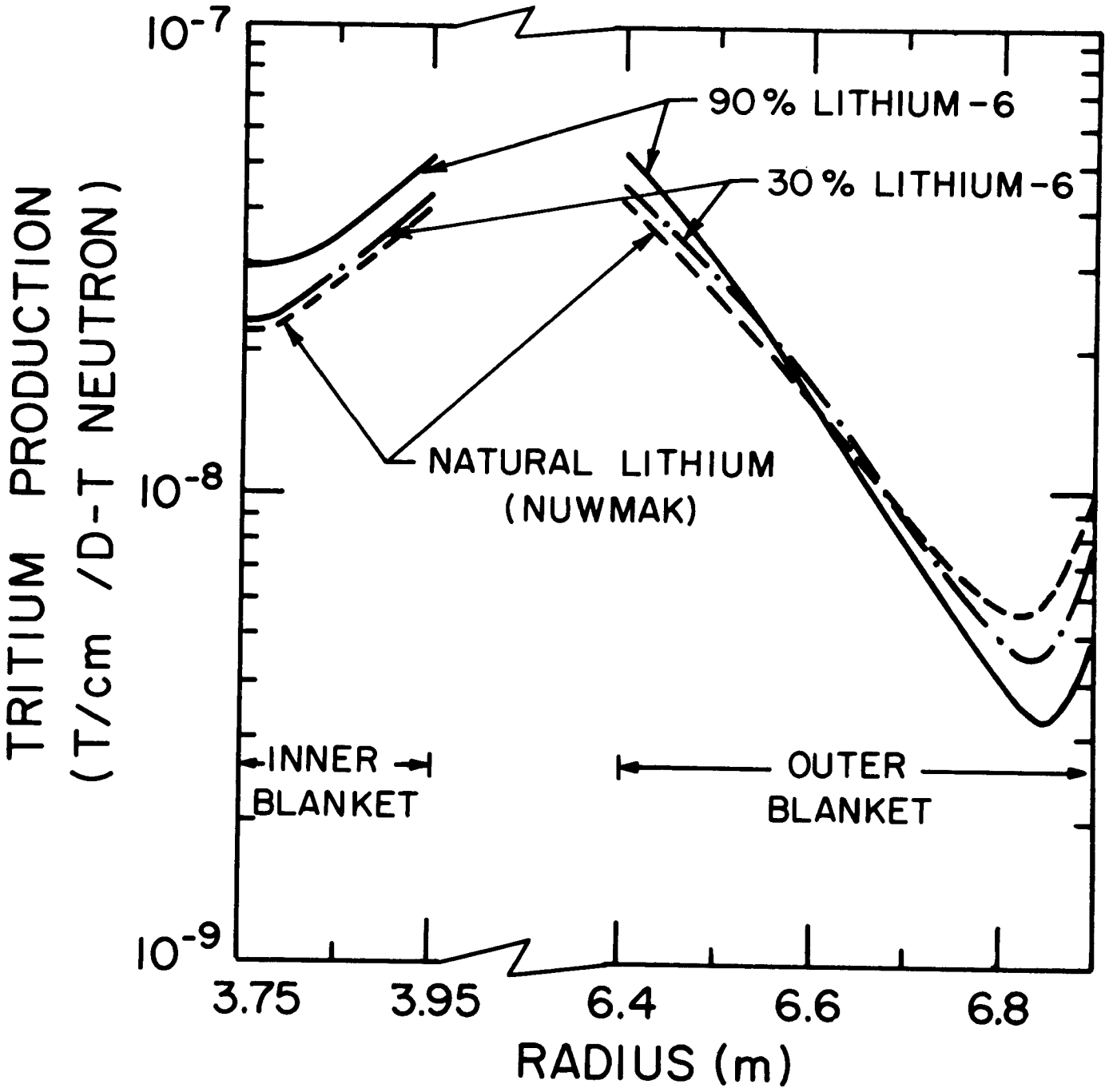
TRITIUM PRODUCTION
(T/cm /D-T NEUTRON)
10^{-7}
10^{-8}
10^{-9}
90% LITHIUM-6
30% LITHIUM-6
NATURAL LITHIUM
(NUWMAK)
INNER
BLANKET
OUTER
BLANKET
3.75
3.95
6.4
6.6
6.8
RADIUS (m)

FIGURE 6

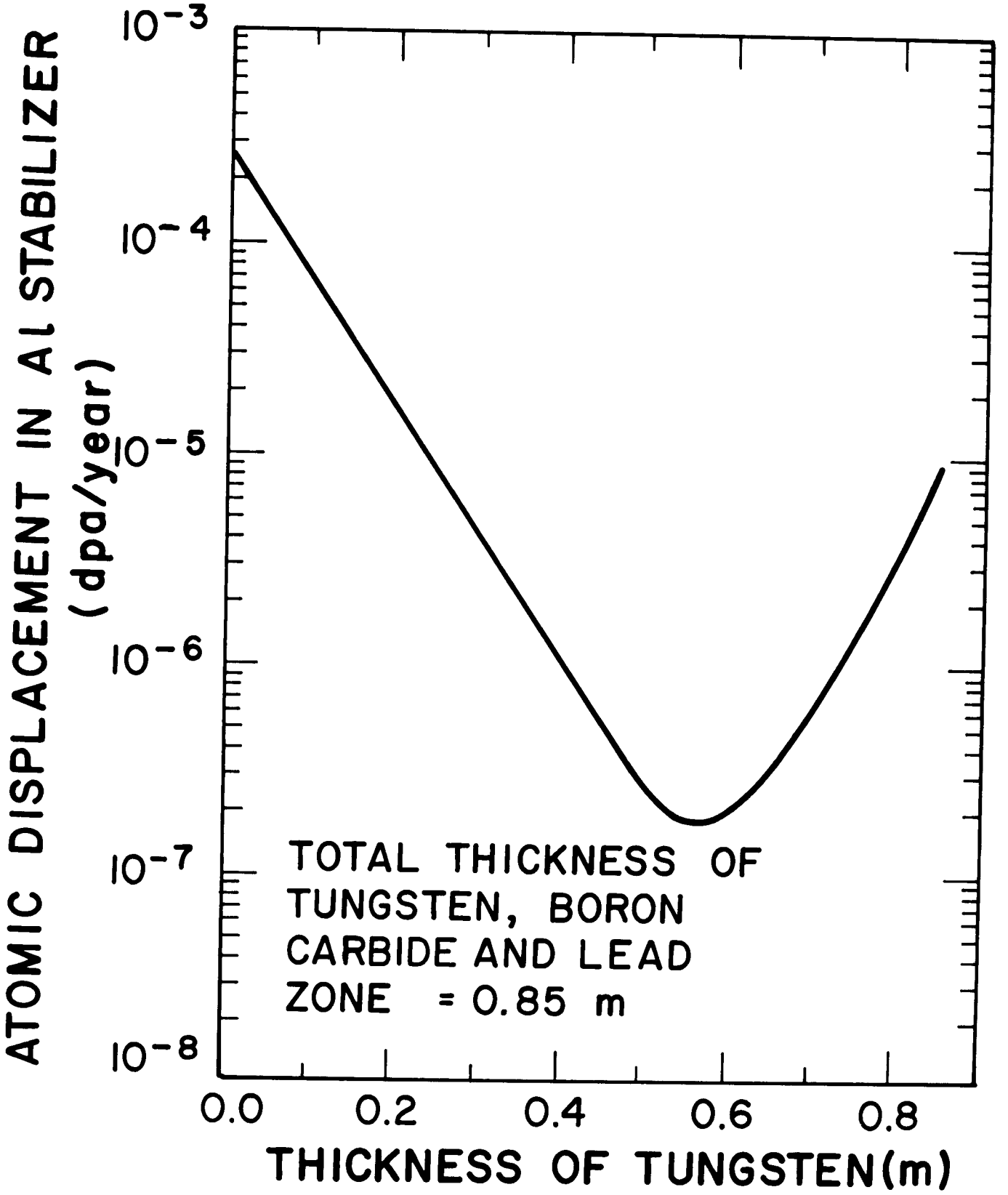
ATOMIC DISPLACEMENT IN Al STABILIZER
(dpa/year)
10-3
10-4
10-5
10-6
10-7
10-8
TOTAL THICKNESS OF
TUNGSTEN, BORON
CARBIDE AND LEAD
ZONE = 0.85 m
0.0
0.2
0.4
0.6
0.8
THICKNESS OF TUNGSTEN(m)

FIGURE 7

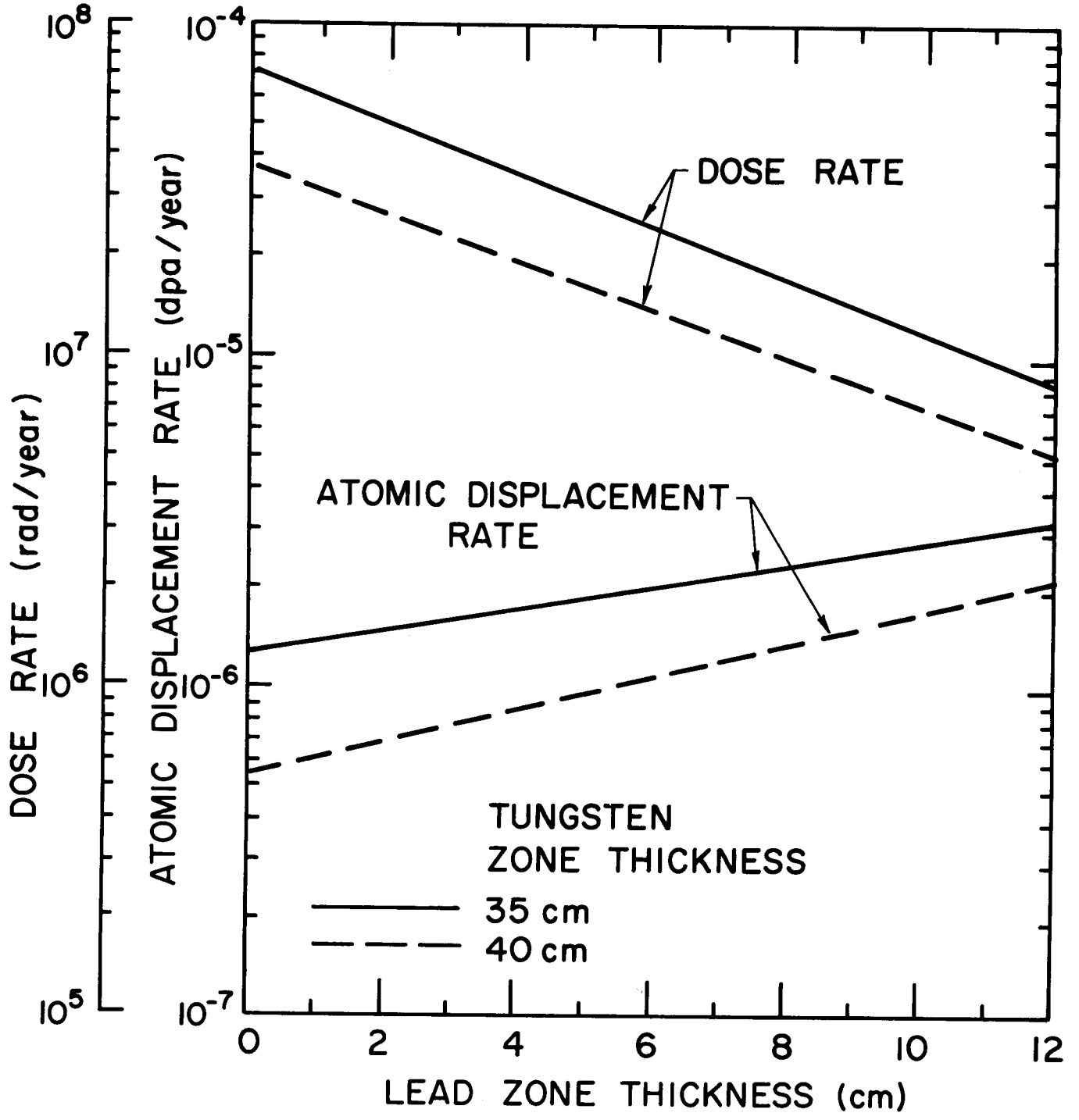
DOSE RATE (rad/year)
ATOMIC DISPLACEMENT RATE (dpa/year)
LEAD ZONE THICKNESS (cm)
DOSE RATE
ATOMIC DISPLACEMENT RATE
TUNGSTEN ZONE THICKNESS
35 cm
40 cm
10^8
10^7
10^6
10^5
10^-4
10^-5
10^-6
10^-7
0
2
4
6
8
10
12

FIGURE 8

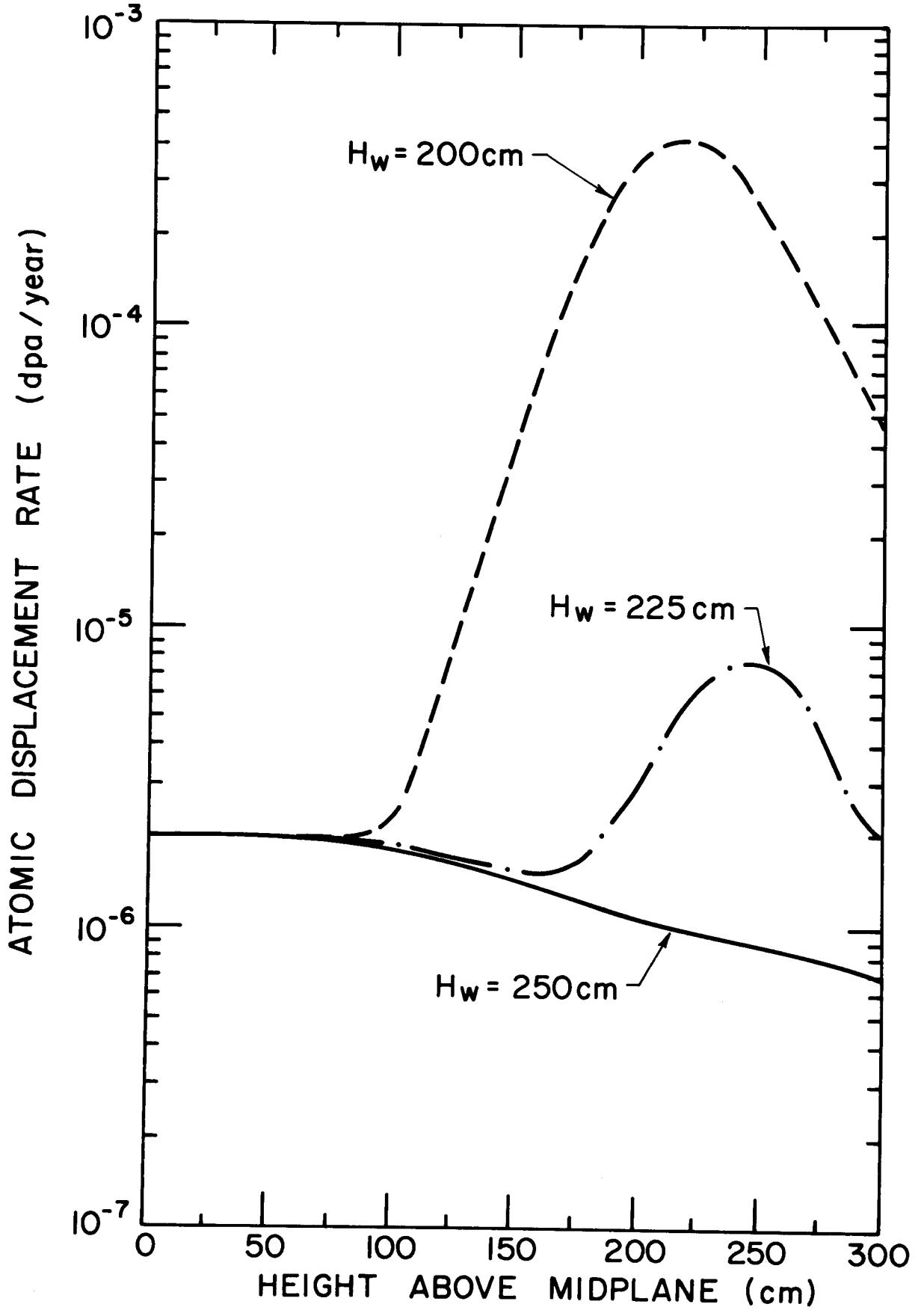
10^{-3}
10^{-4}
10^{-5}
10^{-6}
10^{-7}
ATOMIC DISPLACEMENT RATE (dpa/year)
H_w = 200cm
H_w = 225 cm
H_w = 250cm
0
50
100
150
200
250
300
HEIGHT ABOVE MIDPLANE (cm)

Figure 9

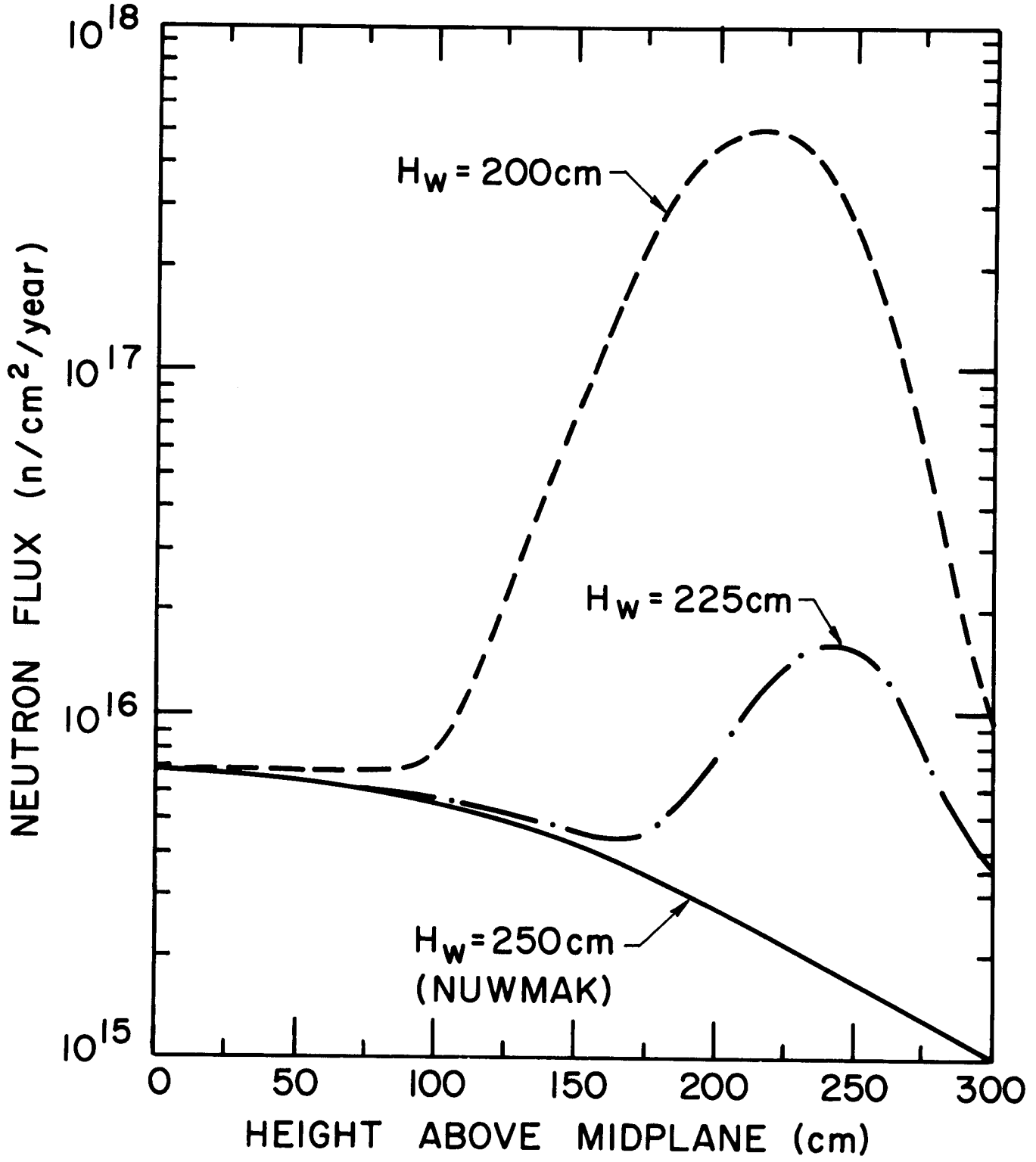
10^{18}
10^{17}
10^{16}
10^{15}
NEUTRON FLUX (n/cm^2/year)
H_w = 200cm
H_w = 225cm
H_w = 250cm
(NUWMAK)
0
50
100
150
200
250
300
HEIGHT ABOVE MIDPLANE (cm)

FIGURE 10

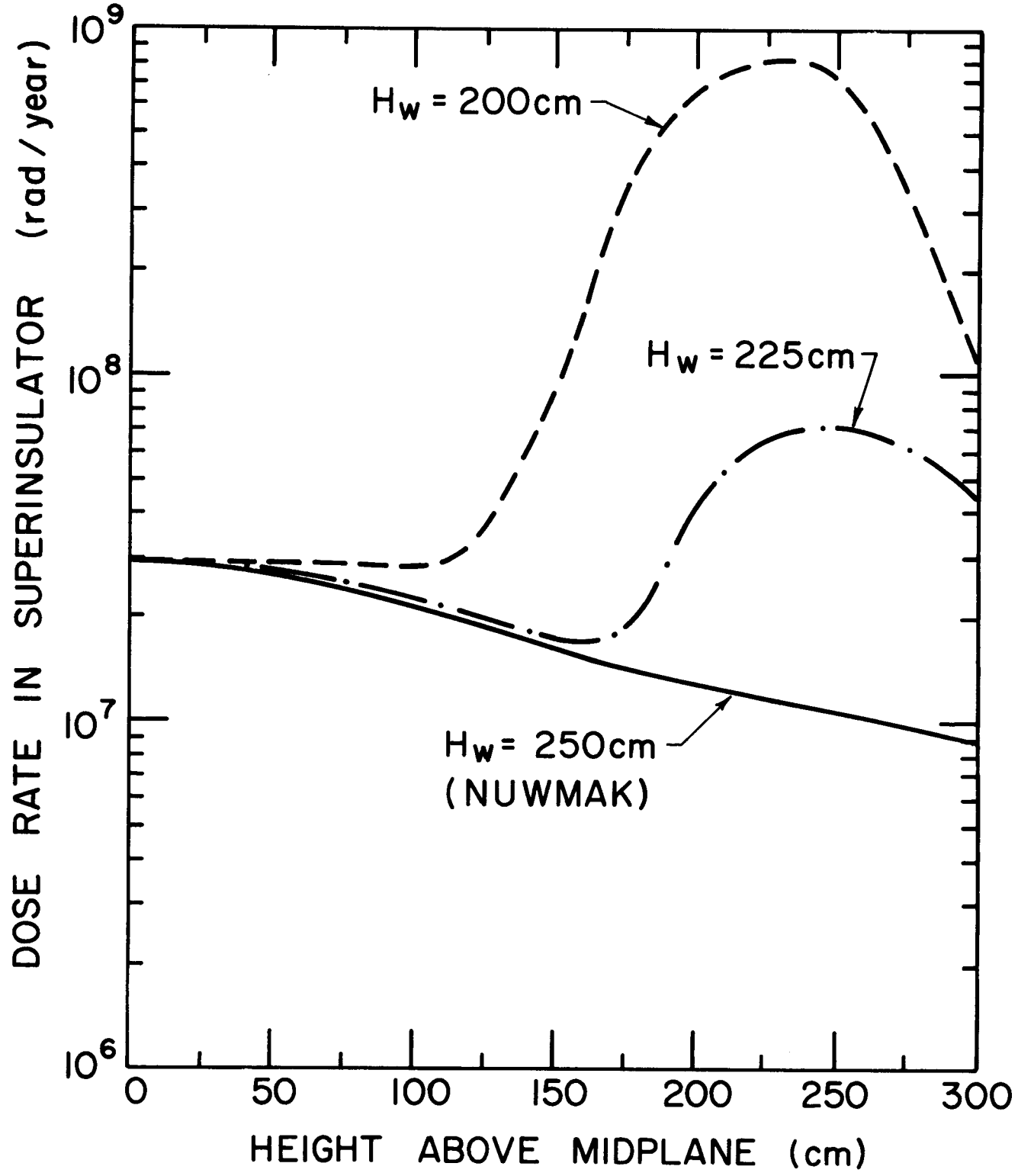
DOSE RATE IN SUPERINSULATOR (rad / year)
10^9
10^8
10^7
10^6
H_w = 200cm
H_w = 225cm
H_w = 250cm
(NUWMAK)
0
50
100
150
200
250
300
HEIGHT ABOVE MIDPLANE (cm)

FIGURE 11

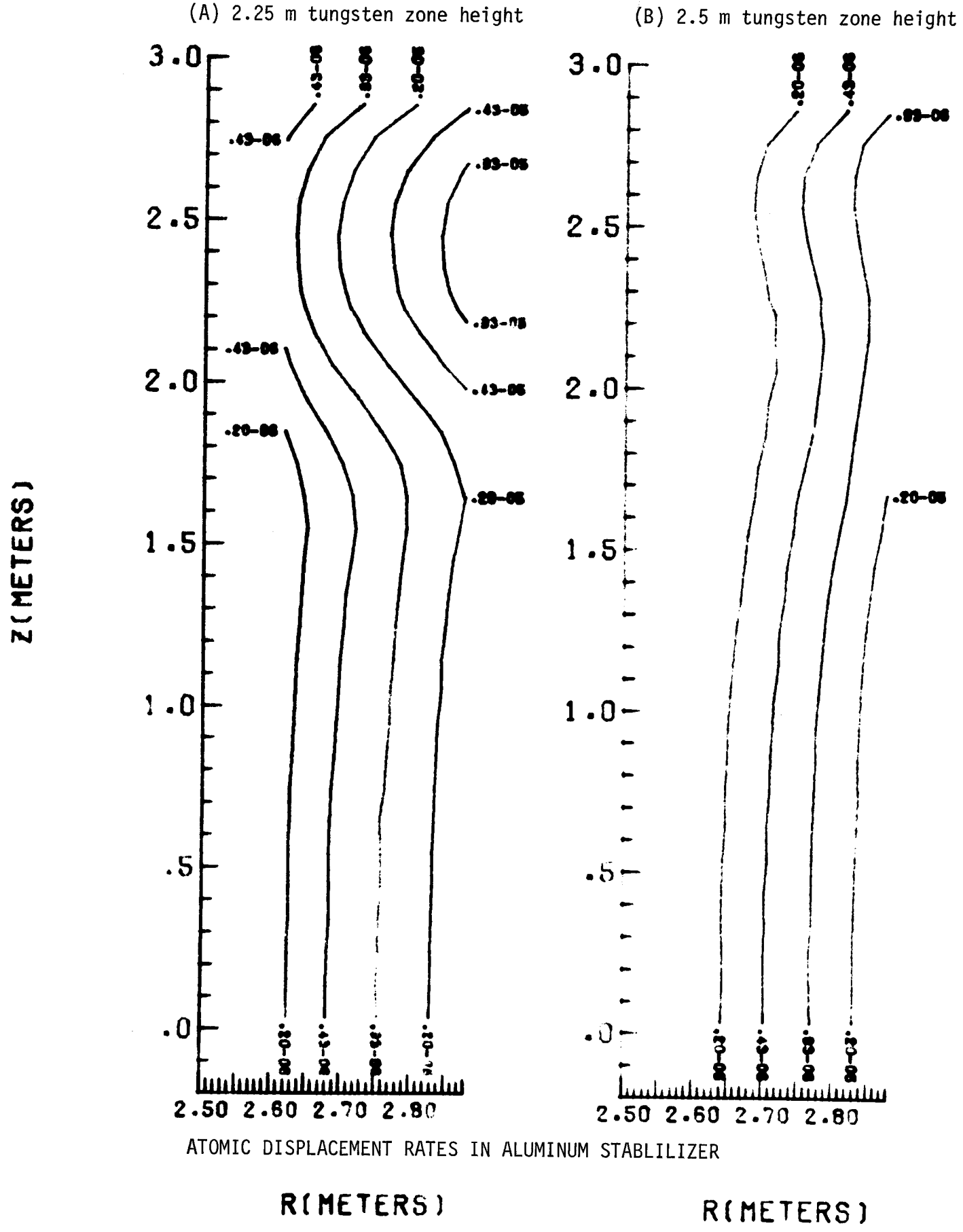

ATOMIC DISPLACEMENT RATES IN ALUMINUM STABLILIZER

FIGURE 12

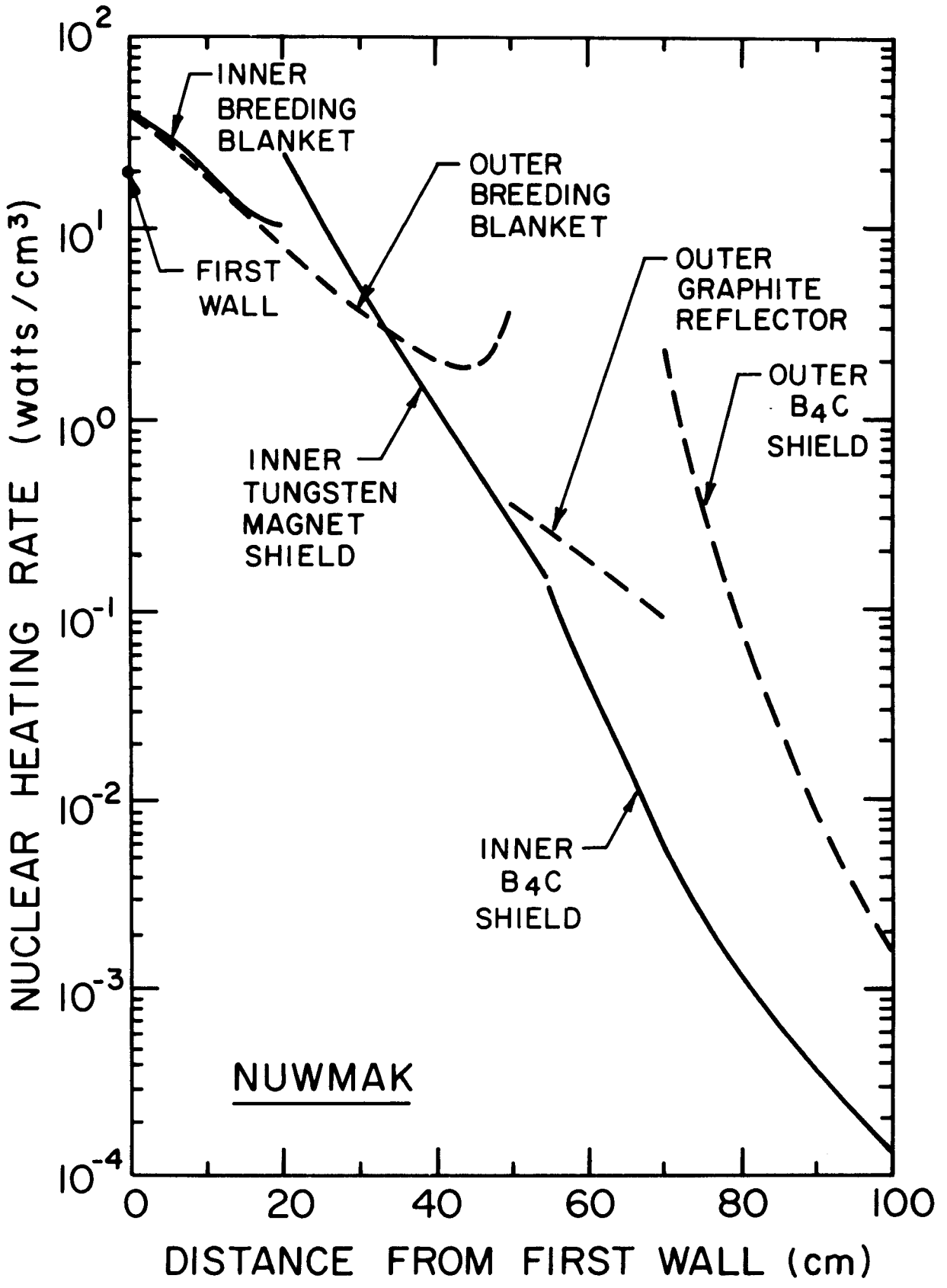
NUCLEAR HEATING RATE (watts/cm³)
DISTANCE FROM FIRST WALL (cm)
INNER BREEDING BLANKET
OUTER BREEDING BLANKET
FIRST WALL
OUTER GRAPHITE REFLECTOR
OUTER B4C SHIELD
INNER TUNGSTEN MAGNET SHIELD
INNER B4C SHIELD
NUWMAK

FIGURE 13

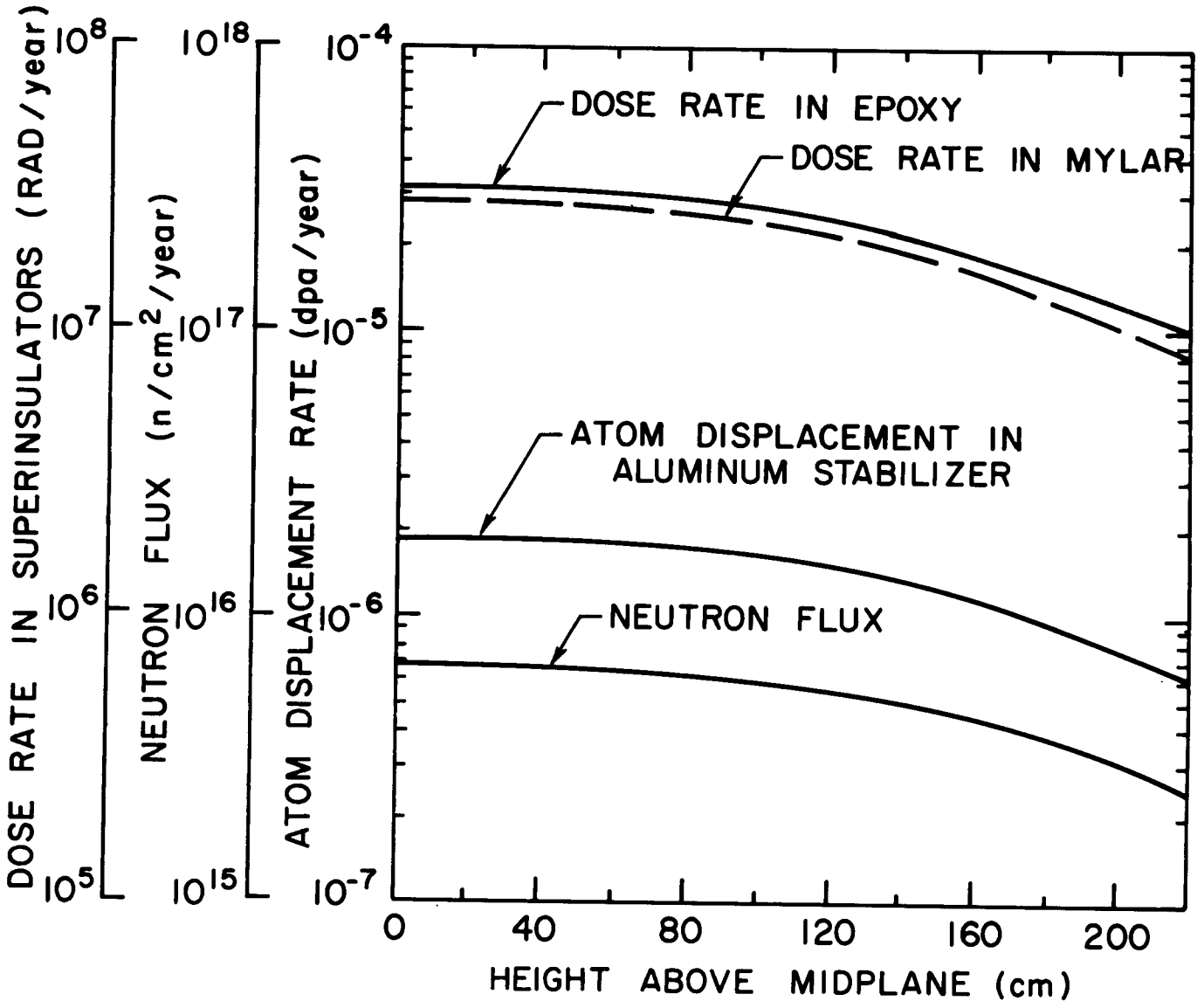
DOSE RATE IN SUPERINSULATORS (RAD/year)
NEUTRON FLUX (n/cm²/year)
ATOM DISPLACEMENT RATE (dpa/year)
10⁸
10⁷
10⁶
10⁵
10¹⁸
10¹⁷
10¹⁶
10¹⁵
10⁻⁴
10⁻⁵
10⁻⁶
10⁻⁷
DOSE RATE IN EPOXY
DOSE RATE IN MYLAR
ATOM DISPLACEMENT IN ALUMINUM STABILIZER
NEUTRON FLUX
0
40
80
120
160
200
HEIGHT ABOVE MIDPLANE (cm)

FIGURE 14

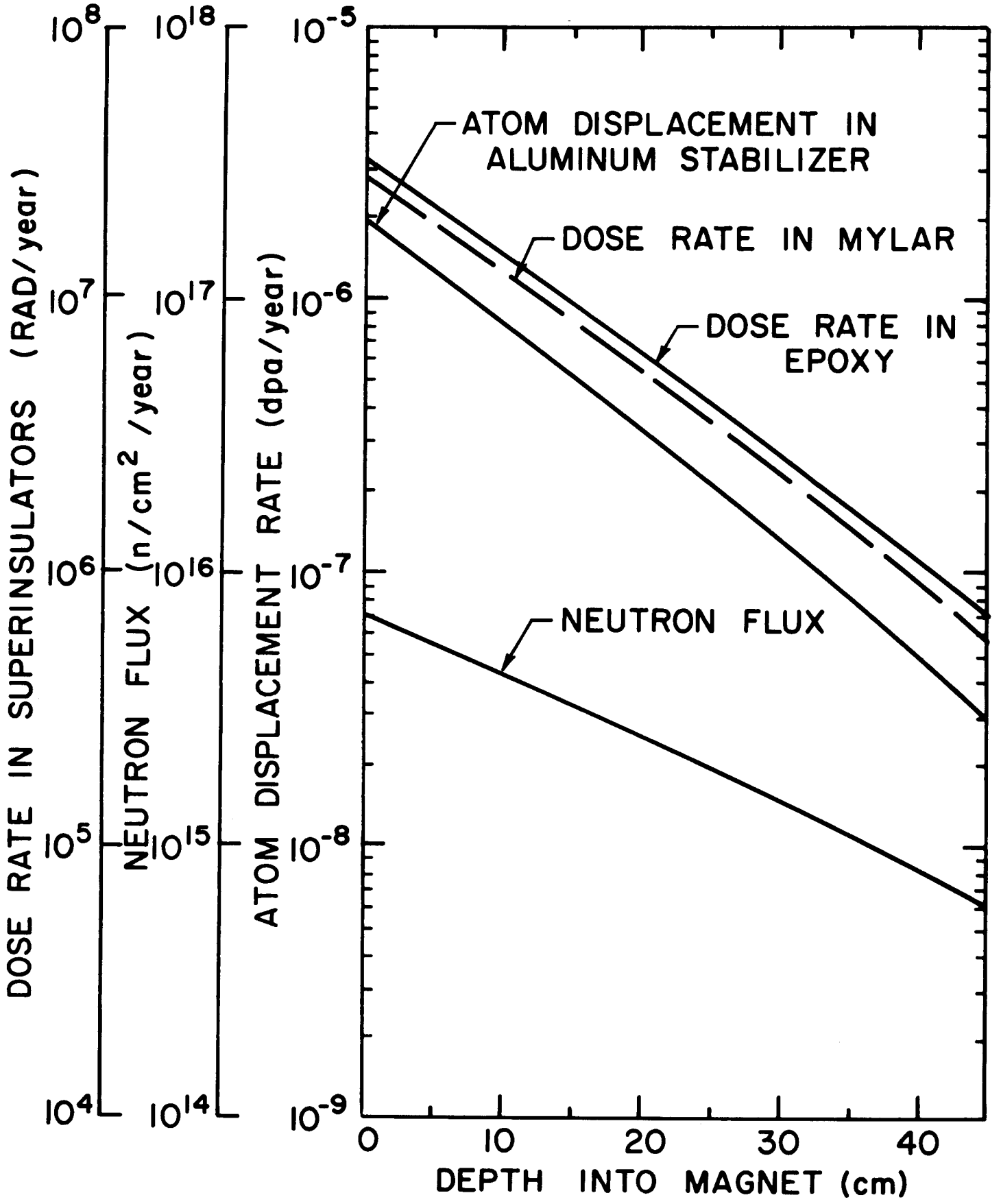
ATOM DISPLACEMENT IN ALUMINUM STABILIZER
DOSE RATE IN MYLAR
DOSE RATE IN EPOXY
NEUTRON FLUX
DOSE RATE IN SUPERINSULATORS (RAD/year)
NEUTRON FLUX (n/cm² /year)
ATOM DISPLACEMENT RATE (dpa/year)
DEPTH INTO MAGNET (cm)
10⁸
10⁷
10⁶
10⁵
10⁴
10¹⁸
10¹⁷
10¹⁶
10¹⁵
10¹⁴
10⁻⁵
10⁻⁶
10⁻⁷
10⁻⁸
10⁻⁹
0
10
20
30
40

FIGURE 15

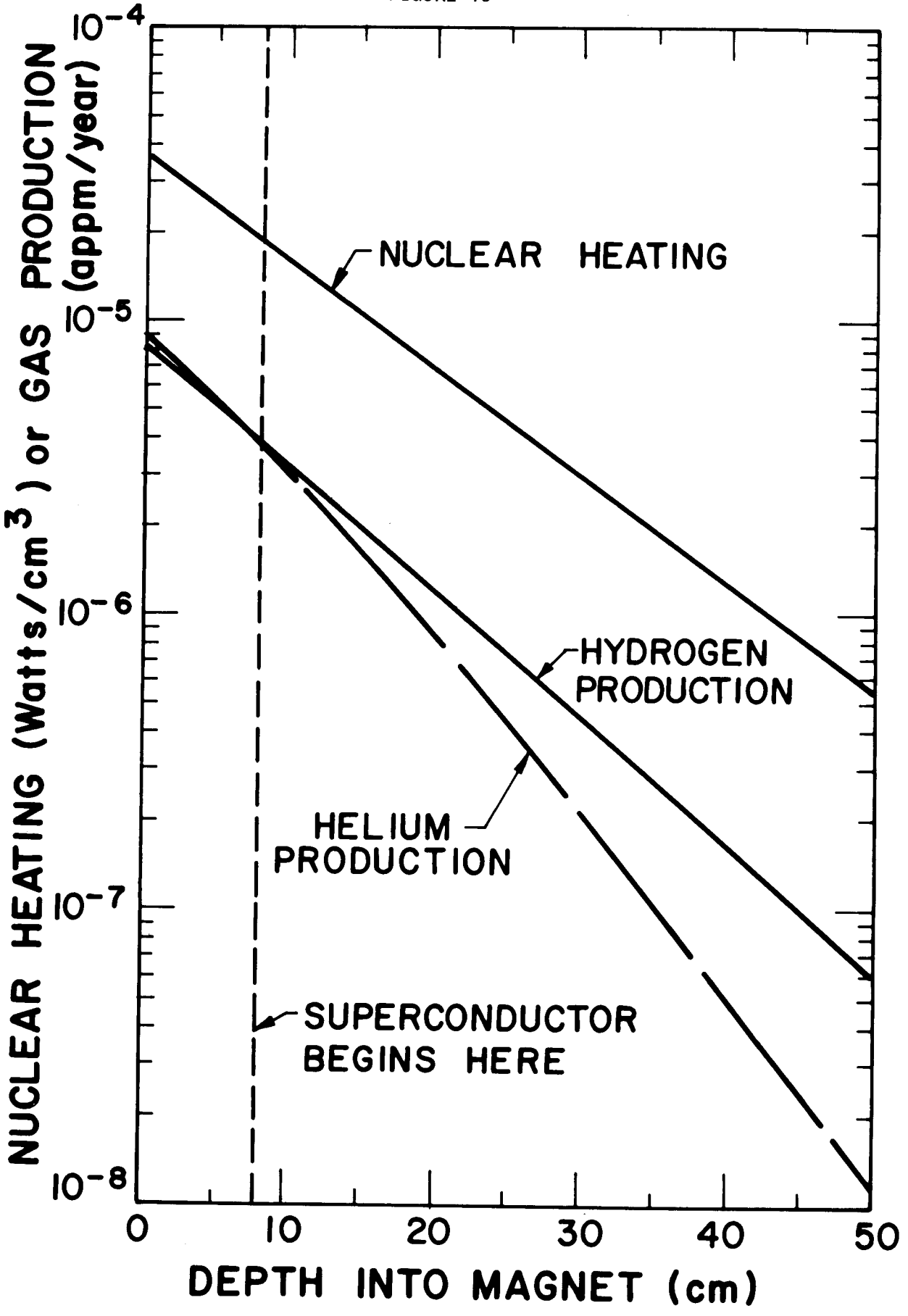
NUCLEAR HEATING (Watts/cm^3) or GAS PRODUCTION (appm/year)
10^{-4}
10^{-5}
10^{-6}
10^{-7}
10^{-8}
NUCLEAR HEATING
HYDROGEN PRODUCTION
HELIUM PRODUCTION
SUPERCONDUCTOR BEGINS HERE
0
10
20
30
40
50
DEPTH INTO MAGNET (cm)

FIGURE 16

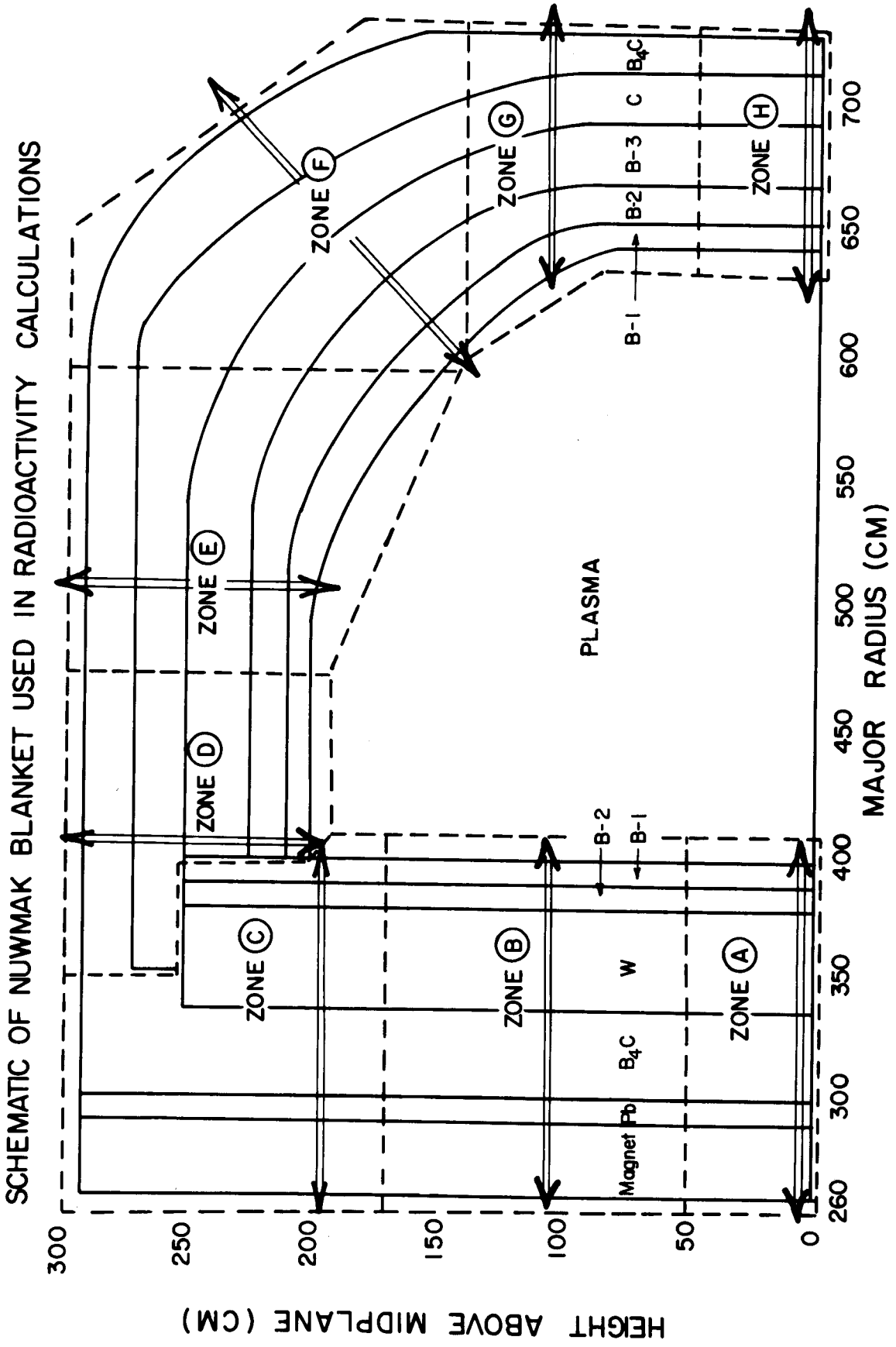
SCHEMATIC OF NUWMAK BLANKET USED IN RADIOACTIVITY CALCULATIONS
ZONE A
ZONE B
ZONE C
ZONE D
ZONE E
ZONE F
ZONE G
ZONE H
PLASMA
W
B_4C
Pb
Magnet
B-1
B-2
B-3
C
MAJOR RADIUS (CM)
HEIGHT ABOVE MIDPLANE (CM)
260
300
350
400
450
500
550
600
650
700
0
50
100
150
200
250
300

FIGURE 17

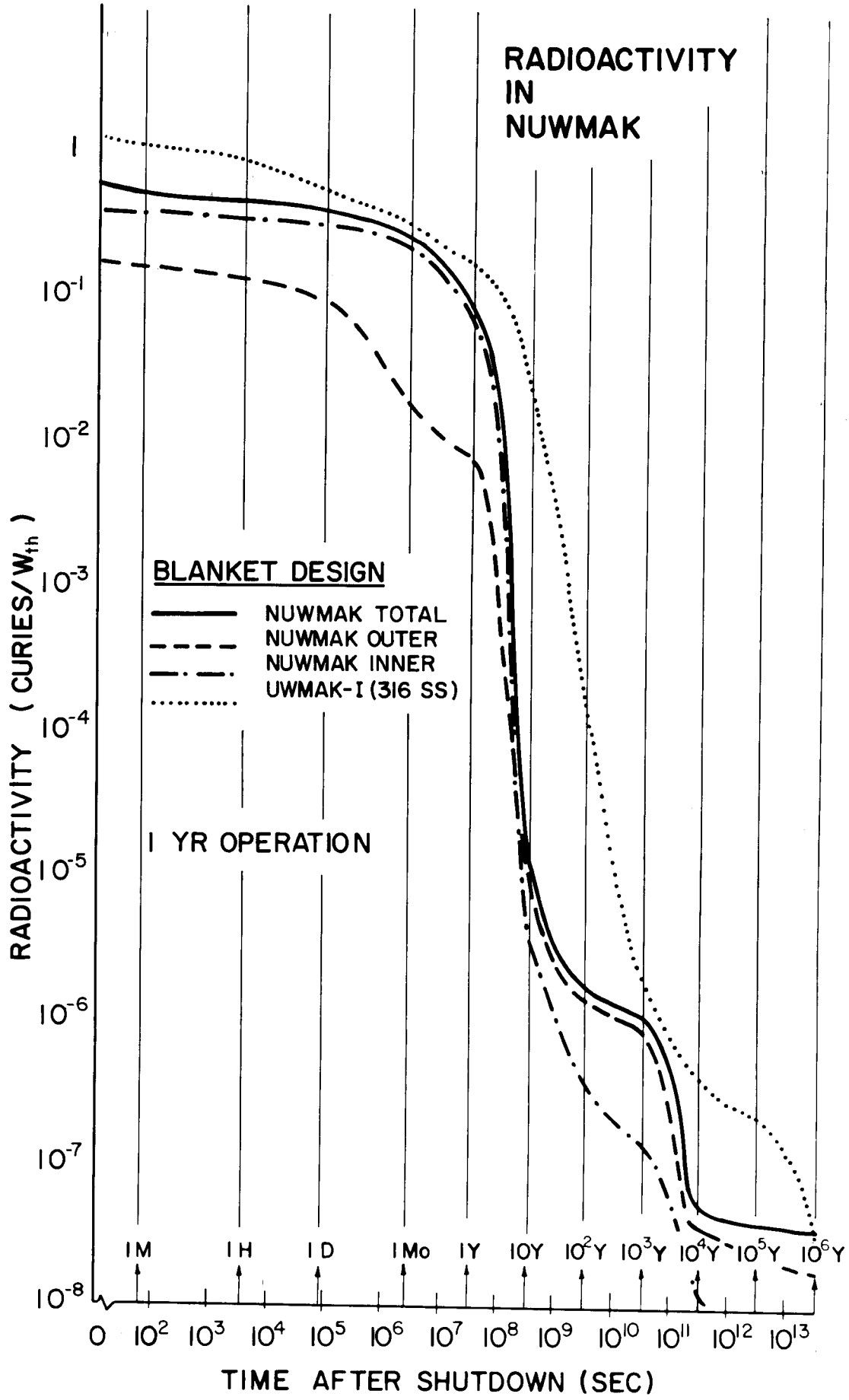
RADIOACTIVITY
IN
NUWMAK
BLANKET DESIGN
NUWMAK TOTAL
NUWMAK OUTER
NUWMAK INNER
UWMAK-I (316 SS)
1 YR OPERATION
RADIOACTIVITY (CURIES/W$_{th}$)
1
10^{-1}
10^{-2}
10^{-3}
10^{-4}
10^{-5}
10^{-6}
10^{-7}
10^{-8}
1M
1H
1D
1Mo
1Y
10Y
10^2Y
10^3Y
10^4Y
10^5Y
10^6Y
0
10^2
10^3
10^4
10^5
10^6
10^7
10^8
10^9
10^{10}
10^{11}
10^{12}
10^{13}
TIME AFTER SHUTDOWN (SEC)

FIGURE 18

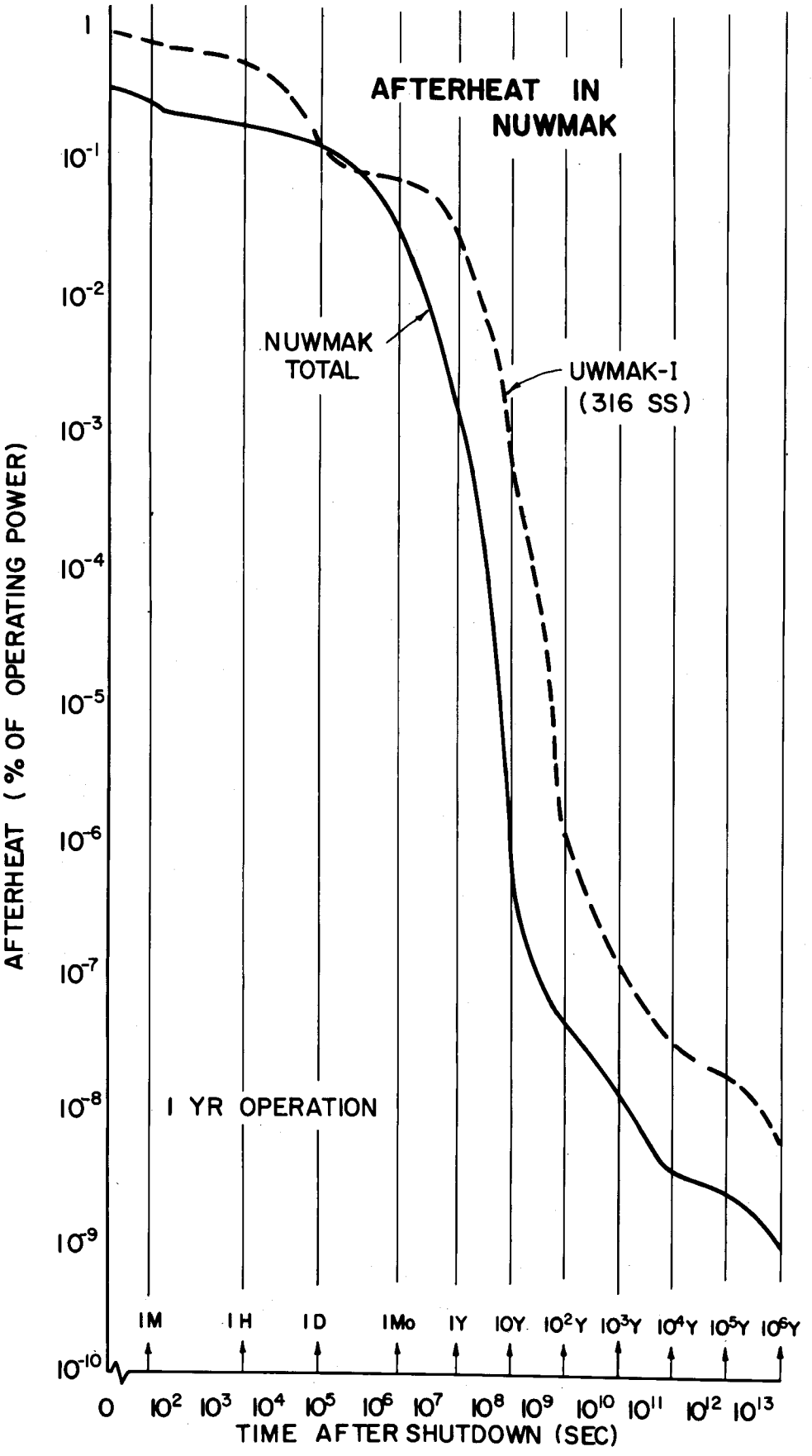
AFTERHEAT IN
NUWMAK
NUWMAK
TOTAL
UWMAK-I
(316 SS)
1 YR OPERATION
AFTERHEAT (% OF OPERATING POWER)
1
10-1
10-2
10-3
10-4
10-5
10-6
10-7
10-8
10-9
10-10
1M
1H
1D
1Mo
1Y
10Y
10²Y
10³Y
10⁴Y
10⁵Y
10⁶Y
0
10²
10³
10⁴
10⁵
10⁶
10⁷
10⁸
10⁹
10¹⁰
10¹¹
10¹²
10¹³
TIME AFTER SHUTDOWN (SEC)

FIGURE 19

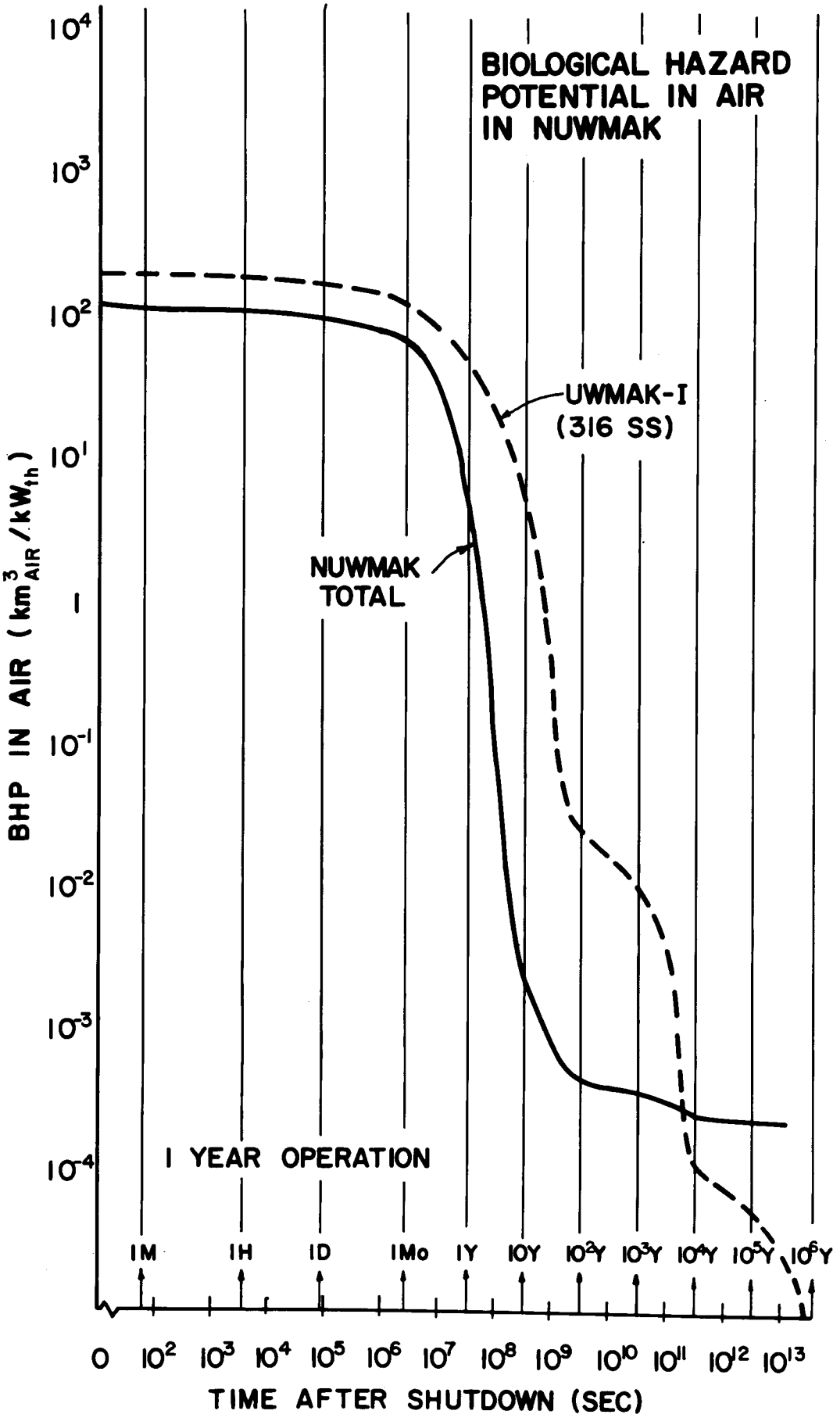
BIOLOGICAL HAZARD
POTENTIAL IN AIR
IN NUWMAK
UWMAK-I
(316 SS)
NUWMAK
TOTAL
1 YEAR OPERATION
BHP IN AIR (km³AIR / kWth)
10⁴
10³
10²
10¹
1
10⁻¹
10⁻²
10⁻³
10⁻⁴
1M
1H
1D
1Mo
1Y
10Y
10²Y
10³Y
10⁴Y
10⁵Y
10⁶Y
0
10²
10³
10⁴
10⁵
10⁶
10⁷
10⁸
10⁹
10¹⁰
10¹¹
10¹²
10¹³
TIME AFTER SHUTDOWN (SEC)